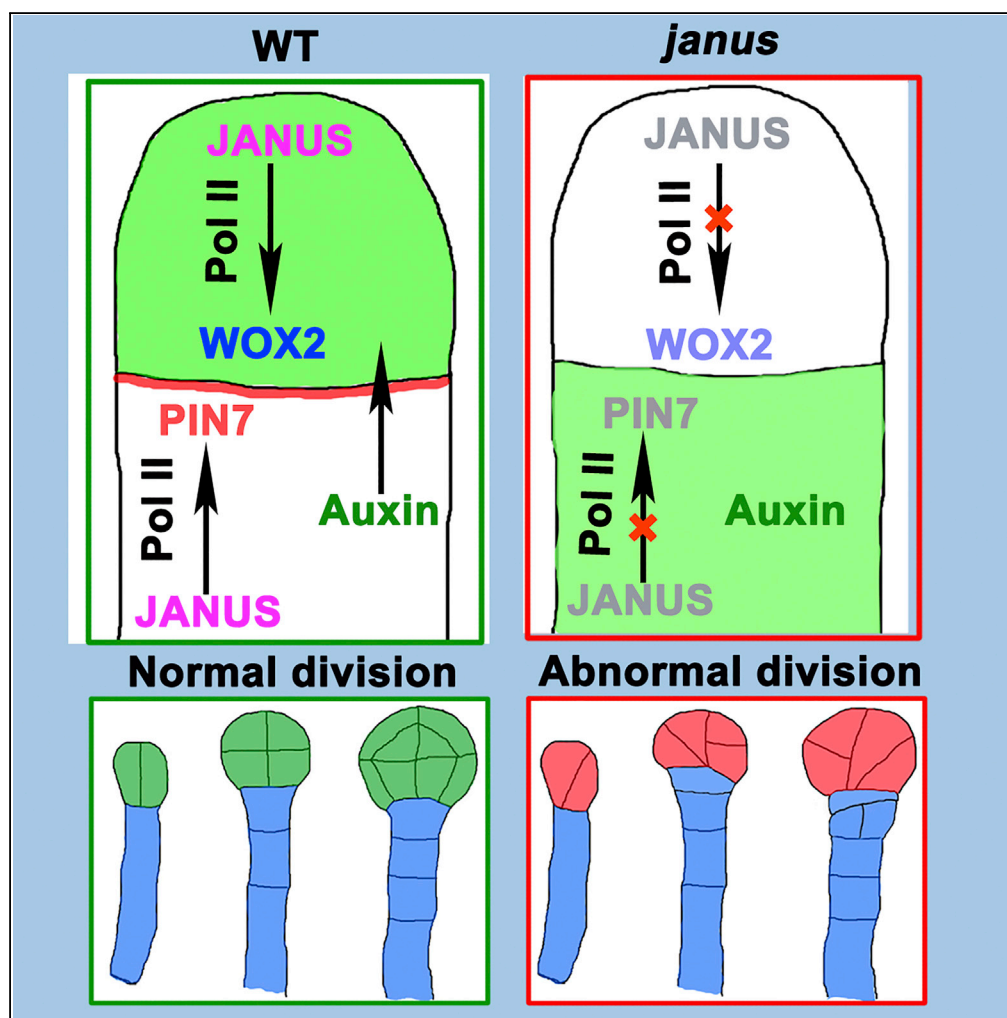**Article**

# Arabidopsis JANUS Regulates Embryonic Pattern Formation through Pol II-Mediated Transcription of *WOX2* and *PIN7*



Feng Xiong, Hai-Hong Liu, Cun-Ying Duan, Bi-Ke Zhang, Guo Wei, Yan Zhang, Sha Li

shali@sdau.edu.cn

**HIGHLIGHTS**

Arabidopsis JANUS, a putative spliceosome subunit, is essential for embryogenesis

JANUS mediates the transcription but not RNA processing of *WOX2* and *PIN7*

JANUS interacts with RNA polymerase II whose mutations caused embryo lethality

Pol II mediates the transcription of *WOX2* and *PIN7* in a JANUS-dependent manner

# iScience

**CellPress**

## Article

# Arabidopsis JANUS Regulates Embryonic Pattern Formation through Pol II-Mediated Transcription of *WOX2* and *PIN7*

Feng Xiong,[1] Hai-Hong Liu,[1] Cun-Ying Duan,[1] Bi-Ke Zhang,[1] Guo Wei,[1] Yan Zhang,[1] and Sha Li[1,2,3,*]

## SUMMARY

**Embryonic pattern formation relies on positional coordination of cell division and specification. Early axis formation during Arabidopsis embryogenesis requires WUSCHEL RELATED HOMEOBOX (WOX)-mediated transcription activation and PIN-FORMED7 (PIN7)-mediated auxin asymmetry. How these events are regulated is obscure. We report that Arabidopsis JANUS, a putative subunit of spliceosome, is essential for embryonic pattern formation. Significantly reduced transcription but not mRNA processing of *WOX2* and *PIN7* in *janus* suggested its role in transcriptional regulation. JANUS interacts with RNA polymerase II (Pol II) through a region outside of its spliceosome-association domain. We further show that Pol II mediates the transcription of *WOX2* and *PIN7* in a JANUS-dependent way and is essential for embryonic pattern formation. These findings reveal that JANUS recruits Pol II for the activation of two parallel pathways to ensure proper pattern formation during embryogenesis.**

## INTRODUCTION

Development of a specific body plan during embryogenesis requires precise cell fate determination based on the position of cells along the embryo axes. In Arabidopsis, the crucial cell types are established extremely early during embryogenesis as reflected by the stereotypic sequence of oriented cell divisions (Lau et al., 2012; ten Hove et al., 2015). Two pathways have been linked to the establishment of apical-basal axis and cell specification after zygotic division. One involves the transcription factors WUSCHEL RELATED HOMEOBOX2 (WOX2), WOX8, and WOX9, whereas the other depends on auxin, whose asymmetry is maintained by auxin efflux carrier PIN-FORMED7 (PIN7) (Lau et al., 2012). *WOX2* and *WOX8* are initially co-expressed in the zygote (Haecker et al., 2004). After zygotic division, *WOX2* and *WOX8* are restricted to the apical and basal cell lineage to control the following cell specification, respectively (Breuninger et al., 2008; Haecker et al., 2004). PIN7 is polarly localized to the apical plasma membrane (PM) of the basal cell, where it provides maternal auxin to the apical cell (Friml et al., 2003; Robert et al., 2018). The polar distribution of PIN7 ensures auxin maximum in the apical cell, which generates the proembryo and all apical structures of the plant. Functional loss of *WOX2* or *PIN7* compromised the formation of apical-basal axis during early embryogenesis. However, their defects at early embryonic pattern formation are later recovered (Friml et al., 2003; Robert et al., 2018). Whether these two pathways play redundant roles in embryogenesis and how their specific expression is controlled are unclear.

RNA polymerase II (Pol II) plays a pivotal role in regulating gene expression (Thomas and Chiang, 2006). Pol II in Arabidopsis consists of 12 core subunits (Ream et al., 2009), in which Nuclear RNA Polymerase B1 (NRPB1) and NRPB2 interact to form the catalytic center for RNA synthesis, whereas other subunits play structural and regulatory roles in transcription initiation, elongation, termination, or RNA processing (Cramer et al., 2008; Werner and Grohmann, 2011). Functional studies of genes encoding for Pol II subunits suggested its role in embryogenesis such that no homozygous mutants could be obtained for functional loss of *NRPB2*, as well as that of *NRPB9* and *NRPB11*, genes encoding for the noncatalytic subunits of Pol II (Onodera et al., 2008; Ream et al., 2009; Tan et al., 2012). However, whether and how functional loss of Pol II affects embryogenesis is unclear.

Spliceosomes are large RNA-protein complexes mainly involved in pre-mRNA splicing. Nevertheless, subunits of spliceosomes also participate in many other processes, including mRNA export (Howard and Sanford, 2015; Muller-McNicoll et al., 2016), the maintenance of genome stability (Li and Manley, 2005; Xiao et al., 2007), and microRNA processing (Ben Chaabane et al., 2013; Wu et al., 2010). Interestingly, reports both in metazoans and in plants showed that a subunit of spliceosome, Serine/arginine-rich splicing
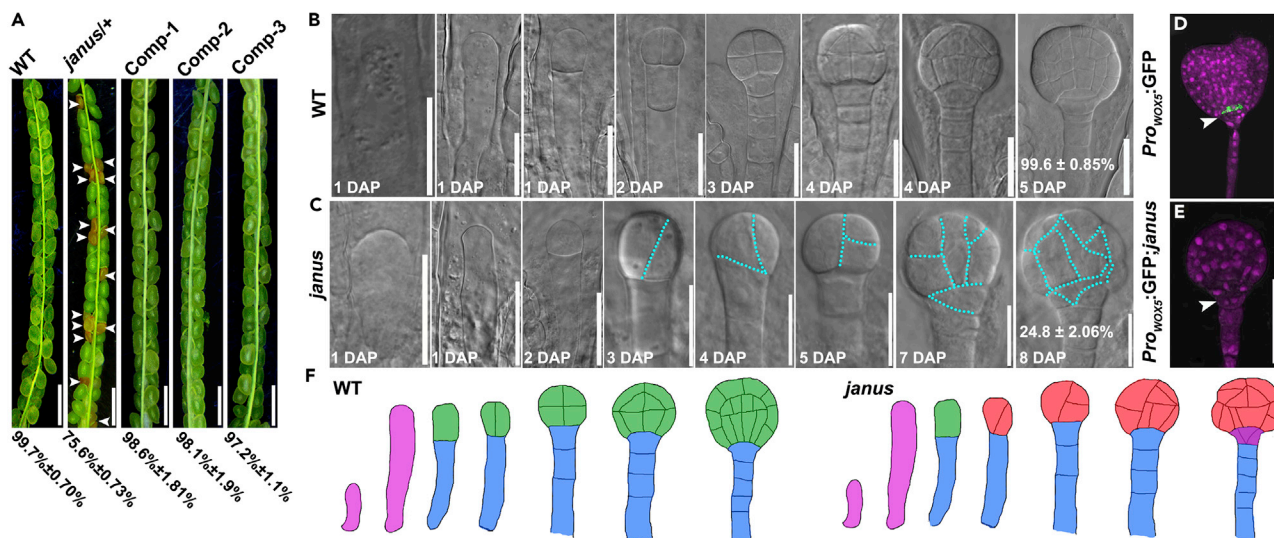
**Figure 1. *JANUS* Is Essential for Pattern Formation during Embryogenesis**

(A) Seed set of different genotypes. Results are means ± standard deviation (SD, n = 8). Seed set of *janus*/+ is significantly different from others (Tukey's multiple comparison test, p < 0.05). Scale bars, 1 mm.

(B and C) Wild-type (WT) and *janus* embryo development by ovule clearing. DAP indicates days after pollination. Because *janus* embryos are much delayed in development, wild-type embryos and *janus* embryos are shown in pairs according to their developmental stages but not to the same DAP. Dotted lines in (C) indicate division planes. Scale bars, 20 μM.

(D and E) Confocal laser scanning microscopy (CLSM) of a $Pro_{WOX5}$:GFP embryo (D) or a $Pro_{WOX5}$:GFP;*janus* embryo (E). Images shown are merges of the GFP channel and RFP channel (propidium iodide [PI] staining in magenta).

(F) Schematic illustration of wild-type or *janus* embryogenesis. Arrowheads point at aborted seeds in (A). The arrowhead points at the Quiescent Center labeled by GFP in (D) but its absence in (E).

factor 35 (SC35), interacts with a Pol II subunit and is required for the transcription of genes, in addition to its role in pre-mRNA splicing (Lin et al., 2008; Yan et al., 2017). A role of the spliceosome subunit in regulating Pol II-mediated transcription was proposed (Yan et al., 2017).

In this study, we report that the Arabidopsis homolog of human SPLICEOSOME-ASSOCIATED PROTEIN 49 (SAP49) and yeast Hsh49p, a subunit of spliceosome, is essential for pattern formation during early embryogenesis. We named it JANUS as it represents the god of new beginnings in ancient Rome and associates with the first steps of a journey. Functional loss of *JANUS* resulted in complete embryo lethality due to abnormal cell division immediately after the first zygotic division. The specific expression of *PIN7* was disrupted in *janus*, resulting in defective auxin signaling. On the other hand, *WOX2* was also transcriptionally downregulated in *janus*. Consistently, the disruption of both *WOX2*- and *PIN7*-dependent pathways resembled pattern formation defects of *janus* during early embryogenesis. We further showed that JANUS interacts with Pol II subunits independent of its role as a splicing factor and is required for Pol II-dependent transcription of *WOX2* and *PIN7*. Indeed, functional loss of Pol II subunits mimicked embryonic defects of *janus*. Taken together, our findings demonstrate that JANUS recruits Pol II to transcriptionally activate WOX2- and PIN7-mediated pathways for pattern formation during early embryogenesis.

## RESULTS

### *JANUS* Is Essential for Pattern Formation during Embryogenesis

*JANUS* was isolated for characterization because of the complete embryo lethality of its mutant *emb2444* (Meinke et al., 2008). JANUS contains two RNA recognition motifs (RRMs) and is homologous to a subunit of the spliceosome (Figures S1A, S1E, and S1F). Segregation ratio from reciprocal crosses between wild-type and *janus*/+ indicated that gametophytic transmission of the mutant was not affected (Table S1). The heterozygous mutant showed one-fourth of seed abortion (Figure 1A). Transcript abundance of *JANUS* was significantly reduced in *janus*/+ compared with that in the wild-type (Figure S1). In addition, the genomic fragment of *JANUS* with a GFP reporter gene in the control of its native promoter was introduced into *janus*/+. Transgenic lines of JANUSg-GFP;*janus* were obtained, and all showed no seed abortion (Figures 1A and S1), indicating that *JANUS* is the causal gene for seed abortion of *janus*.

To determine at which stage developing seeds started to show defects in *janus*, we examined self-fertilized *janus/+* by whole-mount clearing. Embryos developing within a single silique are approximately at the same developmental stage (Breuninger et al., 2008), which enabled an estimate of *janus* embryos, which are much delayed compared with their wild-type siblings. After the first zygotic division, one-fourth of embryos from *janus/+* plants displayed an asymmetric oblique division (Figures 1C and 1F) rather than symmetric vertical division as observed in three-fourth of the other embryos as well as in embryos of the wild-type (Figures 1B and 1F). The division pattern followed was impaired in these presumably *janus* embryos (Figures 1C and 1F), which showed severe morphological defects at the early globular stage and were eventually arrested at the late globular stage (Figures 1C and 1F). In the arrested embryos, the outer walls of protoderm cells were distended, producing an uneven surface on the embryo proper (Figures 1C and 1F). Abnormal divisions occurred both in the apical and the basal lineages (Figures 1C and 1F). Furthermore, the formation and specification of quiescent center (QC) was also compromised judged by the irregularly oblique divisions in hypophysis and by the absence of GFP signals in $Pro_{WOX5}$:GFP;*janus* (Figures 1D and 1E), which specifies the QC (Blilou et al., 2005). These results demonstrated that *JANUS* is an essential gene for early embryonic pattern formation and cell fate specification. Consistent with its role in embryogenesis, *JANUS* is highly expressed in developing embryos from the zygotic stage to the cotyledon stage (Figure S1).

## JANUS Mediates the Expression of *WOX2* and *PIN7*

JANUS is nuclear localized (Figure S1), suggesting a potential role in gene expression. We thus tested whether the two major pathways in controlling early embryogenesis, i.e., WOX-mediated transcriptional pathway and PIN7-mediated auxin signaling pathway, were affected in *janus*. First, we analyzed the transcription activity of *WOX2* and *WOX8* by introducing $Pro_{WOX2}$:DsRed2/$Pro_{WOX8g4}$:NLS-vYFP$_3$ (Yu et al., 2016) in *janus/+*. *WOX2* and *WOX8* were transcriptionally activated in the apical and basal cells after the zygotic division in wild-type, respectively (Figure 2A), as reported (Breuninger et al., 2008; Haecker et al., 2004). By contrast, *WOX2* showed a substantially reduced transcriptional activity in the apical cell lineage of one-fourth embryos in *janus/+*, whereas *WOX8* was not affected (Figures 2A and 2B). The reduced transcription of *WOX2* but not *WOX8* was confirmed by additional reporter line (Figure S2) or native transcript levels (Figure S3). These results suggested that the transcription activity of *WOX2* but not *WOX8* in early embryogenesis depended on *JANUS*.

Second, we examined whether *PIN7* was transcriptionally affected by functional loss of *JANUS*. PIN7 (Blilou et al., 2005) was polarly localized to the apical PM of the basal cells in wild-type globular embryos (Figure 2C), as reported (Friml et al., 2003). In one-fourth embryos from *PIN7:GFP;janus/+*, presumably of the *janus* genotype, GFP signals were significantly reduced or even undetectable (Figure 2C). Because JANUS is homologous to spliceosome subunits (Figure S1), we examined the transcription activity of *PIN7* in $Pro_{PIN7}$:NLS-YFP;*janus/+*, which was reflected by fluorescence intensity, to exclude the possibility that mRNA splicing of *PIN7* contributed to the expression difference. Consistent with the results obtained from *PIN7:GFP*, YFP signals were dramatically reduced or undetectable in the basal cells of one-fourth embryos in $Pro_{PIN7}$:NLS-YFP;*janus/+* (Figure 2D). These results implied that JANUS is crucial for the transcription of *PIN7* during early embryogenesis. Indeed, no splicing defects of *PIN7* as well as of *WOX2* were detected in the siliques of *janus/+* (Figure S2), confirming a role of JANUS in the transcription rather than RNA processing of the two genes. Because PIN7 is critical for auxin polar transport during early embryogenesis (Friml et al., 2003), the reduced PIN7 in *janus* would have severely compromised auxin signaling. It was indeed the case. By examining *DR5:GFP*, a synthetic auxin maximum reporter (Friml et al., 2003), we confirmed that GFP was accumulated in the apical cell lineage immediately after zygotic division and then restricted to the hypophysis of the globular embryos in wild-type plants (Figure 2E), as reported (Friml et al., 2003). By contrast, GFP signals were restricted to the basal cells and failed to establish an apical-basal gradient in one-fourth of embryos in *DR5:GFP;janus/+* (Figure 2E). Similar defects were reported in embryos defective in *PIN7* or treated with auxin efflux inhibitors (Friml et al., 2003).

Finally, we generated a double mutant of *WOX2* and *PIN7* under the rationale that if JANUS mediates the transcriptional activity of *WOX2* and *PIN7* during early embryogenesis, functional loss of both pathways would at least partially mimic the defects of *janus*. Compared with wild-type, the single mutant of *PIN7* or *WOX2*, i.e., *pin7-1* or *wox2-4* (Friml et al., 2003; Zhang et al., 2017), showed a slight defect of apical-axis patterning in early stages during embryogenesis but finally recovered at the globular stage (Figures 2G and 2H), consistent with previous reports (Breuninger et al., 2008; Friml et al., 2003; Haecker et al., 2004). In comparison, the proportion of *wox2-4;pin7-1* embryos with abnormal asymmetric division in early
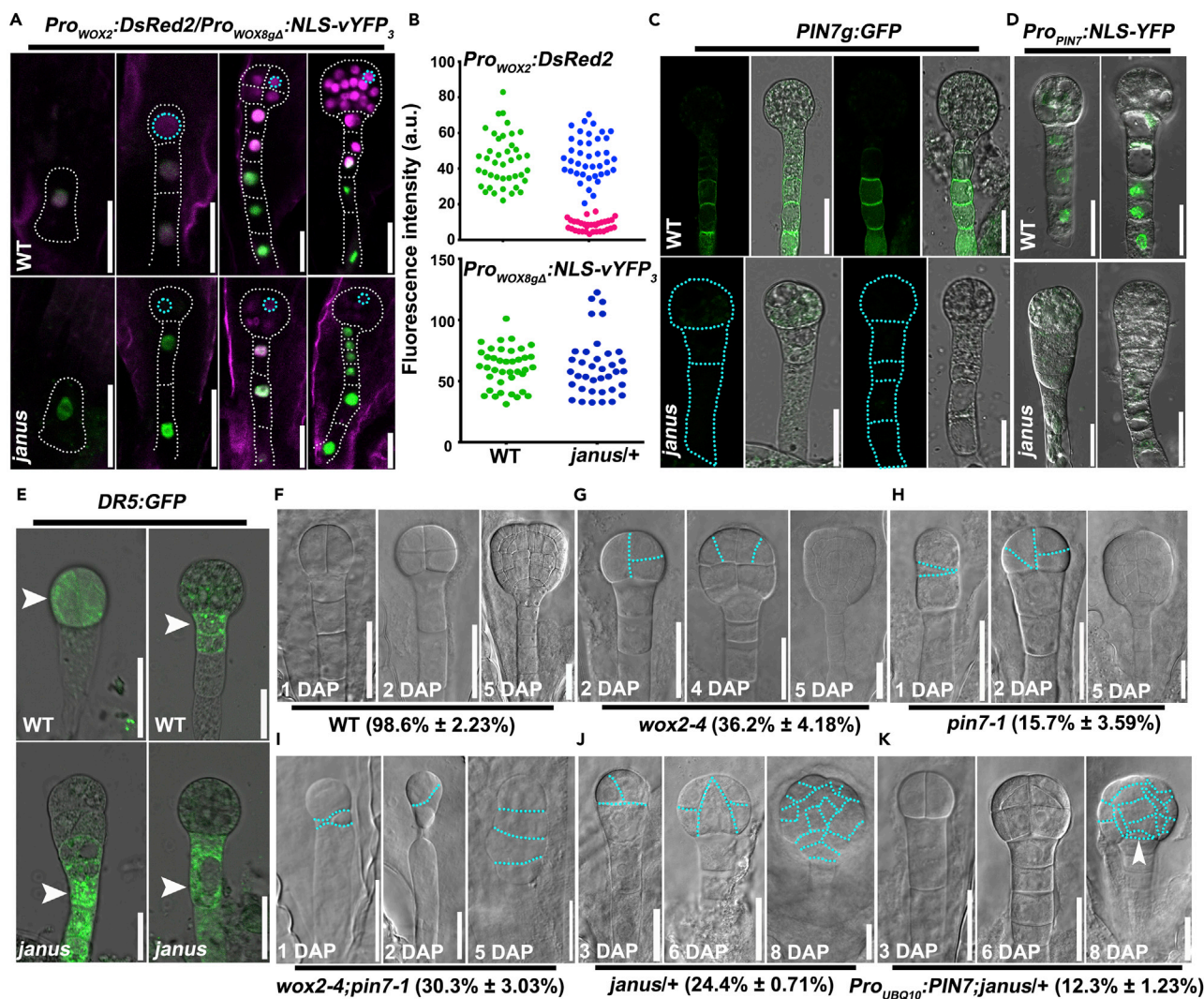
**Figure 2. JANUS Mediates the Expression of *WOX2* and *PIN7***

(A) CLSM of a $Pro_{WOX2}$:DsRed2/$Pro_{WOX8g\Delta}$:NLS-vYFP$_3$ zygote or embryo at early developmental stages either in the wild-type or in *janus* background. Images shown are merges of the RFP (magenta for dsRed) and the GFP (green for NLS-vYFP$_3$) channels. Dotted circles indicate regions of interest (ROI). Scale bars, 20 μM.

(B) Fluorescence intensity of dsRed2 (for $Pro_{WOX2}$) NLS-vYFP$_3$ (for $Pro_{WOX8g\Delta}$). A.u. represents arbitrary fluorescence unit. Results shown are average fluorescence intensities within an ROI. Substantially reduced dsRed2 intensity is indicated in pink, presumably of the *janus* genotype.

(C and D) CLSM of PIN7g:GFP (C) or $Pro_{PIN7}$:NLS-YFP (D) embryos in wild-type or in *janus*. Dotted lines in (C) indicate the silhouettes of the embryo. Scale bars, 20 μM.

(E) CLSM of DR5:GFP embryos in wild-type or in *janus*. Arrowheads point at cells with auxin maximum.

(F–K) WT (F), *wox2-4* (G), *pin7-1* (H), *wox2-4;pin7-1* (I), *janus*/+ (J), or $Pro_{UBQ10}$:PIN7;*janus*/+ (K) embryo development by ovule clearing. Embryos are shown according to their developmental stages but not to the same DAP. Dotted lines indicate division planes. Results are means ± SD (n = 10). The arrowhead in (K) indicates the appearance of the Quiescent Center. In total, 147–404 embryos were examined. Scale bars, 20 μM.

stages substantially increased (Figure 2I). In the wild-type, the first division of the apical cell was vertical and symmetric (Figure 2F), as reported (Breuninger et al., 2008). By contrast, in *wox2-4;pin7-1*, the divisions were asymmetric, either oblique or horizontal in both embryo proper and hypophysis (Figure 2I), which largely resembled those of *janus* during early embryogenesis (Figure 2J). Instead of a full recovery at late stages as seen in each single mutant (Breuninger et al., 2008; Friml et al., 2003; Haecker et al., 2004), over 30% embryos of *wox2-4;pin7-1* arrested immediately after the first zygotic division (Figure 2I). By contrast, enhanced expression of *PIN7* partially complemented the defects of *janus* such that early embryonic pattern formation was largely normal in $Pro_{UBQ10}$:PIN7;*janus*/+ (Figure 2K). These results
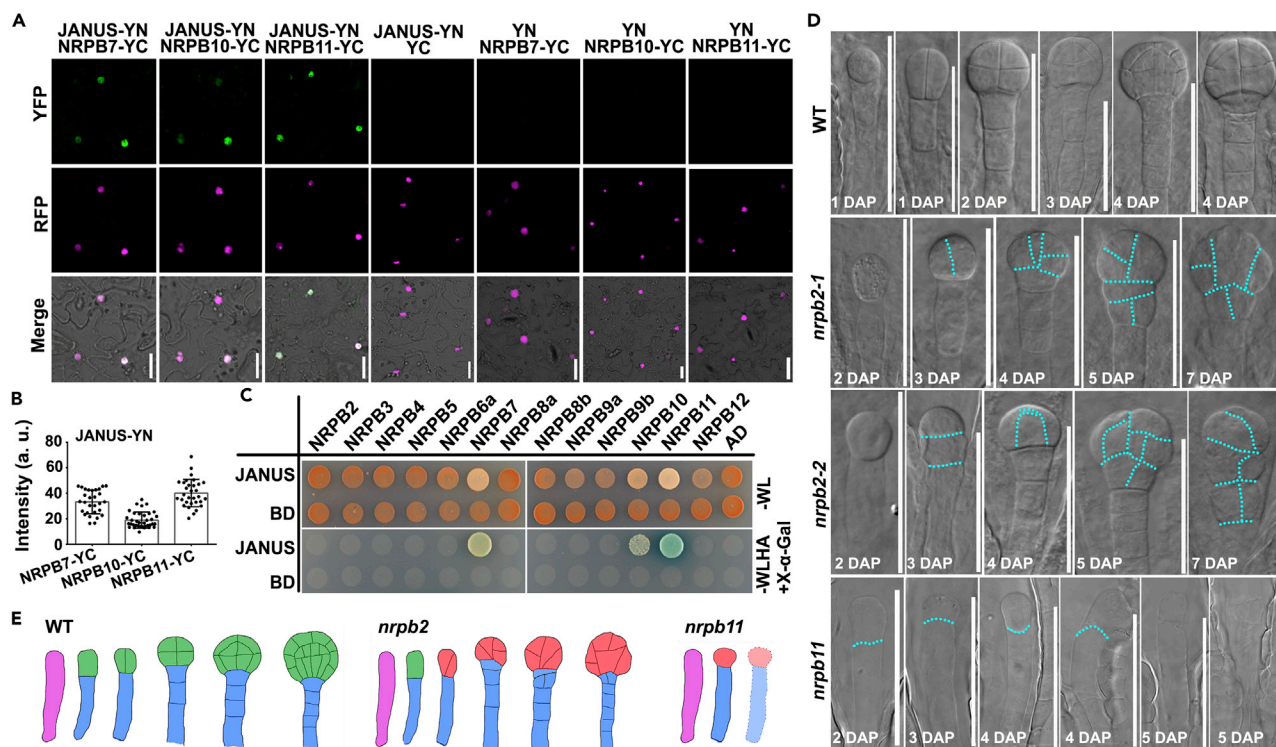
**Figure 3. JANUS Interacts with Pol II whose Functional Loss Resulted in Embryo Lethality**

(A) Bimolecular complementation (BiFC) assays demonstrating the interaction between three Pol II subunits and JANUS. YFP signals are shown in green. U1-70k is used as a nuclear marker (magenta). Scale bars, 20 μM.

(B) Quantification of BiFC signals based on fluorescence intensity within nuclei. Results are means ± SD.

(C) Yeast two hybrid (Y2H) assays showing the interaction between three Pol II subunits and JANUS. Diploid yeast strains are grown on medium lacking Trp and Leu (-WL). Positive interactions are determined by growth on medium lacking Trp, Leu, His, Ade, and supplemented with X-α-Gal (-WLHA + X-α-Gal). Results are representative of three biological replicates.

(D) WT, nrpb2-1, nrpb2-2, or nrpb11 embryo development by ovule clearing. Embryos are shown according to their developmental stages but not to the same DAP. Dotted lines indicate division planes. Scale bars, 50 μM.

(E) Schematic illustration of wild-type, nrpb2, or nrpb11 embryogenesis.

suggested that both WOX2- and PIN7-dependent pathways may be transcriptionally regulated by JANUS and play redundant roles in apical-basal patterning during early embryogenesis.

## JANUS Interacts with Pol II Whose Functional Loss Resulted in Embryo Lethality

To determine how JANUS affected the transcription activity of *WOX2* and *PIN7* during embryonic pattern formation, we tested whether JANUS interacted with components of Pol II since Pol II is responsible for the transcription of most mRNAs in eukaryotes (Thomas and Chiang, 2006) and was shown to interact with other components of the spliceosome (Yan et al., 2017). Of 11 Pol II subunits tested, NRPB7, NRPB10, and NRPB11 showed interaction with JANUS by yeast two hybrid (Y2H) and bimolecular fluorescence complementation (BiFC) assays (Figures 3A–3C and S4). Interestingly, the interaction is evolutionarily conserved: JANUS homolog also interacts with Pol II components in mice (Figure S4).

The physical interaction between JANUS and Pol II suggested that they might function in the same pathway. Indeed, all three genes are highly expressed during embryogenesis based on reporter analysis (Figure S4). We thus hypothesized that functional loss of Pol II would also result in defective embryonic pattern formation. To test this hypothesis, we characterized mutants of NRPB10 and NRPB11, both of which interact with JANUS (Figure S4). Although NRPB7 also interacts with JANUS, the lack of its mutants in all stock centers prevented further analysis. Likely due to the redundancy with *NRPB10*-like genes (Ream et al., 2015), functional loss of *NRPB10* did not show seed set reduction and embryo lethality (Figure S4). In comparison, functional loss of *NRPB11*, a single gene in Arabidopsis (Ream et al., 2015), resulted in embryo lethality (Figure S4), similar to nrpb2 (Onodera et al., 2008). Because both genes are required for Pol II activity (Kershnar et al., 1998;

Ream et al., 2009), these results hinted at an essential role of Pol II in embryogenesis. To identify the defects of embryogenesis due to Pol II loss of function, we examined developing embryos in *nrpb2-1/+*, *nrpb2-2/+*, and *nrpb11-1/+*. The apical-basal patterning during early embryogenesis was significantly affected in one-fourth of *nrpb11-1/+* as well as in 29% of the *nrpb2/+* mutants (Figures 3D and 3E). Similar to that in *janus*, the first division of the apical cell, i.e., symmetric and horizontal in wild-type, was asymmetric and oblique in *nrpb11* and *nrpb2* (Figures 3D and 3E). Irregular division patterns resulted in abnormal formation of embryo proper and hypophysis (Figures 3D and 3E). In most severe cases, embryos were arrested at as early as the two-cell stage (Figures 3D and 3E). Thus, these results demonstrated that Pol II is essential for early embryonic pattern formation and likely functions in the same genetic pathway as JANUS.

### Pol II-Mediated *WOX2* and *PIN7* Transcription Depends on *JANUS*

That JANUS interacts with Pol II and affects the transcription activity of *WOX2* and *PIN7* suggested that Pol II might mediate *WOX2* and *PIN7* transcription during embryonic pattern formation in a JANUS-dependent way. We thus hypothesized that functional loss of Pol II would compromise *WOX2* and *PIN7* expression during early embryonic pattern formation. To test this hypothesis, we introduced $Pro_{WOX2}$:*GFP* and *PIN7:GFP* into *nrpb2-1/+* and examined the fluorescence distribution during embryogenesis. Indeed, the expression of *WOX2* and *PIN7* was severely reduced or even undetectable in one-fourth embryos of the *nrpb2-1/+* plants (Figures 4A and 4B), reminiscent of that in *janus/+*. Auxin signaling was also compromised during early embryogenesis by functional loss of *NRPB2* such that ectopic GFP signals were detected in the basal cells of one-fourth *DR5:GFP;nrpb2-1/+* embryos (Figure 4C), similar to that by functional loss of *JANUS*. These results suggested that Pol II mediates the transcription of *WOX2* and *PIN7* during early embryonic pattern formation.

To test whether Pol II-mediated transcription of *WOX2* and *PIN7* depended on JANUS, we examined Pol II occupancy at the promoter regions of *WOX2* and *PIN7* by chromatin immunoprecipitation (ChIP) using an antibody against NRPB2 (Yan et al., 2017). Because no homozygous *janus* plants could be obtained, we generated $Pro_{35S}$:*JANUS-RNAi* transgenic plants. Transcript analysis as well as fluorescence quantification supported a significant reduction of *JANUS* by RNAi in $Pro_{35S}$:*JANUS-RNAi* transgenic plants (Figure S5). ChIP assays indicated that Pol II occupancy was significantly reduced at the promoter regions of *PIN7* in $Pro_{35S}$:*JANUS-RNAi* lines (Figures 4F and 4G) as compared with that in the wild-type (Figures 4F and 4G). Consistent with the reduced Pol II occupancy, *PIN7* was transcriptionally downregulated in $Pro_{35S}$:*JANUS-RNAi* lines, either by quantitative PCRs for the endogenous genes (Figures 4J and 4K) or by fluorescence quantification of the *PIN7:GFP* transgenic plants (Figures 4D, 4E, 4H, and 4I). Except for embryos, *WOX2* was weakly expressed in a few cells at root maturation zone (Figure 4D), which hindered the application of ChIP assays on its promoter regions. However, by analyzing the fluorescence in the $Pro_{35S}$:*JANUS-RNAi*;$Pro_{WOX2}$:*H2B-GFP* or $Pro_{WOX2}$:*DsRed2;janus/+* plants, we confirmed that JANUS-RNAi or *janus* significantly reduced the transcription activity of $Pro_{WOX2}$ (Figures 2A and 4D). These results suggested that Pol II-mediated transcription of *WOX2* and *PIN7* depends on JANUS. By contrast, the transcription of *WOX8* and *SCARECROW* (*SCR*), a critical embryonic gene (Wysocka-Diller et al., 2000), depends on Pol II but not *JANUS* (Figure S3), suggesting that JANUS did not affect the transcriptional activity of Pol II in general.

## DISCUSSION

Early embryogenesis is the critical developmental phase during which the basic features of the plant body are established. Although distinct expression domains of WOX family transcription factors as well as directional auxin transport are known to be involved in early apical-basal patterning, their upstream regulators and potential interactions were obscure. Our results demonstrated that the two pathways control early embryonic pattern formation in a parallel way and both mediated by JANUS. First, functional loss of *WOX2* and *PIN7* caused a severe defect immediately after the zygotic division, which cannot be restored at late stages, unlike the disruption of each pathway. Second, both *WOX2* and *PIN7* were transcriptionally downregulated by *JANUS* loss of function. The effect of *JANUS* on *PIN7* and *WOX2* is specific because *WOX8*, another embryonic gene, requires RNA Pol II but not JANUS for its expression during early embryogenesis. Third, *wox2-4;pin7-1* resembled *janus* in early embryogenesis. Finally, the accumulation of Pol II at *PIN7* was significantly reduced by JANUS-RNAi, suggesting JANUS-dependent recruitment of the transcriptional machinery at *PIN7*.

Although transcription and RNA processing are coupled *in vivo* (Bentley, 2002; Hirose and Manley, 2000; Lee and Tarn, 2013; Proudfoot et al., 2002; Yan et al., 2017), studies have proven that splicing factors may interact
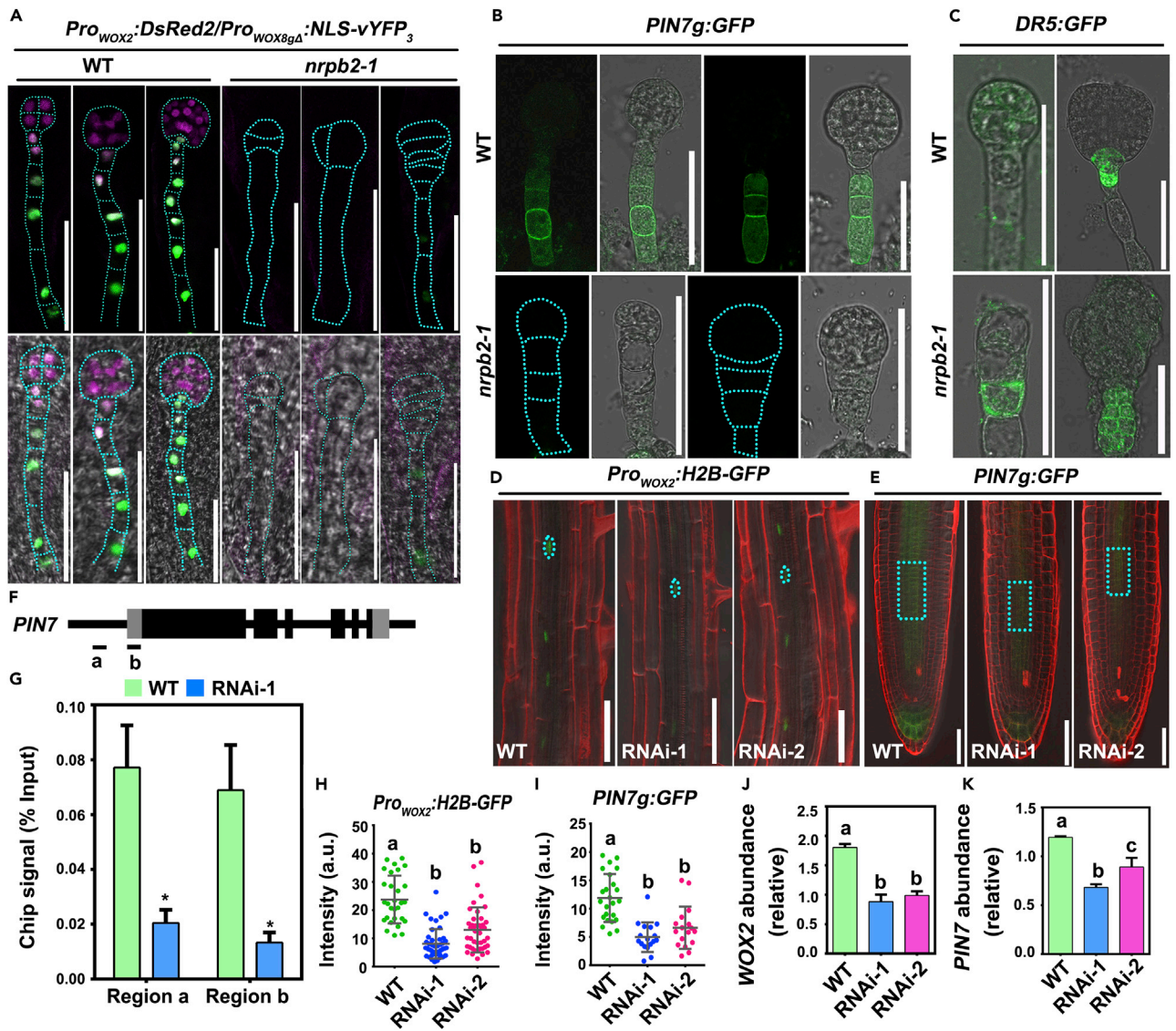
**Figure 4. Pol II-mediated *WOX2* and *PIN7* Transcription Depends on *JANUS***

(A) CLSM of $Pro_{WOX2}$:DsRed2/$Pro_{WOX8g4}$:NLS-vYFP$_3$ embryos at early developmental stages either in the wild-type or in *nrpb2-1* background. Images shown on top are merges of the RFP (magenta for dsRed) and the GFP (green for NLS-vYFP) channels; on bottom are merges of the RFP, GFP, and transmission channels. Dotted lines indicate the silhouettes of the embryo. Scale bars, 50 μM.

(B and C) CLSM of PIN7g:GFP (B) or DR5:GFP (C) embryos in wild-type or in *nrpb2-1*. Dotted lines indicate the silhouettes of the embryo. Scale bars, 50 μM.

(D and E) CLSM of $Pro_{WOX2}$:H2B-GFP (D) or PIN7g:GFP (E) in wild-type or in two lines of $Pro_{35S}$:JANUS-RNAi. Dotted circles indicate ROI. Scale bars, 20 μM.

(F) Schematic representation of the structure of PIN7. The letters indicate the positions of primer pairs used for ChIP-PCR.

(G) Quantification data of the ChIP results. ChIP-PCRs were used to analyze the Pol II enrichment at *PIN7*, which is presented as ratio of (Pol II *PIN7*/input *PIN7*) to (Pol II *Actin*/input *Actin*). Results are means ± standard error (SEM) from three technical repeats. ChIP assays were repeated three times with similar results. Asterisks indicate significant difference (t test, $p < 0.05$).

(H and I) Intensity of H2B-GFP (for $Pro_{WOX2}$) (H) or PIN7g:GFP (I). Results shown are average fluorescence intensities within an ROI, shown in (D) and (E), respectively. Different letters indicate significantly different groups (Tukey's multiple comparison test, $p < 0.05$).

(J and K) Relative transcript abundance of *WOX2* (J) or *PIN7* (K). Results shown are means ± SD (n = 3). Different letters indicate significantly different groups (Tukey's multiple comparison test, $p < 0.05$). Three biological replicates were examined with similar results.

with transcription machinery to directly influence gene expression in metazoans (Braunschweig et al., 2013; Das et al., 2007). Although we cannot exclude a role of JANUS in RNA splicing owing to its homology to the component of the spliceosome during embryogenesis, results presented here strongly suggested its role through transcriptional regulation. First, *JANUS* is critical for the transcription but not RNA splicing of

*WOX2* and *PIN7*, two genes critical for early embryonic pattern formation. Second, the RRM1 domain of yeast SAP49 or metazoan Hsh49p, homolog of Arabidopsis JANUS, is responsible for RNA binding and spliceosome association and is essential for spliceosome-mediated RNA splicing (Igel et al., 1998; Kuwasako et al., 2017; Pauling et al., 2000; van Roon et al., 2017). However, we found that JANUS directly interacts with Pol II through its RRM2 but not RRM1 domain, suggesting that its interaction with Pol II does not require its association with the spliceosome. Third, yeast and metazoan homologs of JANUS are part of an SF3b complex within the spliceosome (Kuwasako et al., 2017; van Roon et al., 2017). However, although other components of the SF3b complex in Arabidopsis have been functionally characterized (Aki et al., 2011; Wang and Brendel, 2006), none of the related mutants showed embryo lethality.

Eukaryotes decode their genomes using three essential nuclear DNA-dependent RNA polymerases (Cramer et al., 2008; Werner and Grohmann, 2011). In Arabidopsis, several subunits of Pol II, including NRPB2, NRPB5, NRPB9, and NRPB11, have been reported to affect plant viability (Onodera et al., 2008; Ream et al., 2009; Tan et al., 2012). However, whether and how Pol II regulates embryogenesis was unclear. We showed here that mutations at a few Pol II components resulted in complete embryo lethality (Figures 3D and S3I). A few components of Pol II are shared by two plant-specific RNA polymerase complexes, Pol IV and Pol V (Ream et al., 2009). However, we believe that Pol II is key for JANUS-mediated transcription of *WOX2* and *PIN7* because the JANUS-interacting component NRPB7 is specific for Pol II (Figures 3A and S3B) and only Pol II was reported to be essential for viability (Herr et al., 2005; Kanno et al., 2005; Onodera et al., 2005; Pontier et al., 2005; Ream et al., 2009).

Data presented here suggested that *JANUS* is important for the Pol II-mediated transcription of *WOX2* and *PIN7* during early embryogenesis. However, JANUS has no recognizable DNA-binding domains. It is unclear how JANUS determines the selectivity of Pol II on target genes such as *WOX2* and *PIN7*. In eukaryotes, mediators, multi-subunit complexes, bridge transcription activators with Pol II at specific *cis*-elements for transcription initiation (Dolan and Chapple, 2017). Whether JANUS fulfills a role of mediator, recruiting DNA-binding transcription factors together with Pol II, to the promoter regions of *WOX2* and *PIN7*, is an interesting scenario worthy of further investigation.

### Limitations of the Study

We would like to note that, because both *janus* and Pol II mutants are embryo lethal, some molecular and biochemical experiments can only be carried out in $Pro_{35S}$:JANUS-RNAi plants. Future efforts will be dedicated to generate weak mutant alleles of *JANUS*, for which homozygous plants can be used for further mechanistic analysis. We also would like to point out that, although *JANUS* is important for Pol II-mediated transcription of *WOX2* and *PIN7* during early embryogenesis, it is unclear how JANUS, a protein containing no DNA-binding domains, determines target selectivity for Pol II. Whether JANUS contains untraditional DNA-binding domains or interacts with transcription factors for its function will be interesting scenario for future studies.

### METHODS

All methods can be found in the accompanying Transparent Methods supplemental file.

### SUPPLEMENTAL INFORMATION

Supplemental Information can be found online at https://doi.org/10.1016/j.isci.2019.09.004.

### AUTHOR CONTRIBUTIONS

Conceptualization, F.X.; Methodology, F.X.; Investigation, F.X., H.-H.L., C.-Y.D., B.-K.Z., and G.W.; Writing – original draft, F.X.; Writing – review and editing, Y.Z. and S.L.; Supervision, Y.Z. and S.L.; Funding acquisition, Y.Z. and S.L.

## DECLARATION OF INTERESTS

The authors declare no competing interests.

## REFERENCES

Aki, S., Nakai, H., Aoyama, T., Oka, A., and Tsuge, T. (2011). AtSAP130/AtSF3b-3 function is required for reproduction in *Arabidopsis thaliana*. Plant Cell Physiol. *52*, 1330–1339.

Ben Chaabane, S., Liu, R., Chinnusamy, V., Kwon, Y., Park, J.H., Kim, S.Y., Zhu, J.K., Yang, S.W., and Lee, B.H. (2013). STA1, an *Arabidopsis* pre-mRNA processing factor 6 homolog, is a new player involved in miRNA biogenesis. Nucleic Acids Res. *41*, 1984–1997.

Bentley, D. (2002). The mRNA assembly line: transcription and processing machines in the same factory. Curr. Opin. Cell Biol. *14*, 336–342.

Blilou, I., Xu, J., Wildwater, M., Willemsen, V., Paponov, I., Friml, J., Heidstra, R., Aida, M., Palme, K., and Scheres, B. (2005). The PIN auxin efflux facilitator network controls growth and patterning in *Arabidopsis* roots. Nature *433*, 39–44.

Braunschweig, U., Gueroussov, S., Plocik, A.M., Graveley, B.R., and Blencowe, B.J. (2013). Dynamic integration of splicing within gene regulatory pathways. Cell *152*, 1252–1269.

Breuninger, H., Rikirsch, E., Hermann, M., Ueda, M., and Laux, T. (2008). Differential expression of WOX genes mediates apical-basal axis formation in the *Arabidopsis* embryo. Dev. Cell *14*, 867–876.

Cramer, P., Armache, K.-J., Baumli, S., Benkert, S., Brueckner, F., Buchen, C., Damsma, G., Dengl, S., Geiger, S., and Jasiak, A. (2008). Structure of eukaryotic RNA polymerases. Annu. Rev. Biophys. *37*, 337–352.

Das, R., Yu, J., Zhang, Z., Gygi, M.P., Krainer, A.R., Gygi, S.P., and Reed, R. (2007). SR proteins function in coupling RNAP II transcription to pre-mRNA splicing. Mol. Cell *26*, 867–881.

Dolan, W.L., and Chapple, C. (2017). Conservation and divergence of mediator structure and function: insights from plants. Plant Cell Physiol. *58*, 4–21.

Friml, J., Vieten, A., Sauer, M., Weijers, D., Schwarz, H., Hamann, T., Offringa, R., and Jurgens, G. (2003). Efflux-dependent auxin gradients establish the apical-basal axis of *Arabidopsis*. Nature *426*, 147–153.

Haecker, A., Gross-Hardt, R., Geiges, B., Sarkar, A., Breuninger, H., Herrmann, M., and Laux, T. (2004). Expression dynamics of WOX genes mark cell fate decisions during early embryonic patterning in *Arabidopsis thaliana*. Development *131*, 657–668.

Herr, A.J., Jensen, M.B., Dalmay, T., and Baulcombe, D.C. (2005). RNA polymerase IV

directs silencing of endogenous DNA. Science *308*, 118–120.

Hirose, Y., and Manley, J.L. (2000). RNA polymerase II and the integration of nuclear events. Genes Dev. *14*, 1415–1429.

Howard, J.M., and Sanford, J.R. (2015). The RNAissance family: SR proteins as multifaceted regulators of gene expression. Wiley Interdiscip. Rev. RNA *6*, 93–110.

Igel, H., Wells, S., Perriman, R., and Ares, M., Jr. (1998). Conservation of structure and subunit interactions in yeast homologues of splicing factor 3b (SF3b) subunits. RNA *4*, 1–10.

Kanno, T., Huettel, B., Mette, M.F., Aufsatz, W., Jaligot, E., Daxinger, L., Kreil, D.P., Matzke, M., and Matzke, A.J. (2005). Atypical RNA polymerase subunits required for RNA-directed DNA methylation. Nat. Genet. *37*, 761–765.

Kershnar, E., Wu, S.Y., and Chiang, C.M. (1998). Immunoaffinity purification and functional characterization of human transcription factor IIH and RNA polymerase II from clonal cell lines that conditionally express epitope-tagged subunits of the multiprotein complexes. J. Biol. Chem. *273*, 34444–34453.

Kuwasako, K., Nameki, N., Tsuda, K., Takahashi, M., Sato, A., Tochio, N., Inoue, M., Terada, T., Kigawa, T., Kobayashi, N., et al. (2017). Solution structure of the first RNA recognition motif domain of human spliceosomal protein SF3b49 and its mode of interaction with a SF3b145 fragment. Protein Sci. *26*, 280–291.

Lau, S., Slane, D., Herud, O., Kong, J., and Jurgens, G. (2012). Early embryogenesis in flowering plants: setting up the basic body pattern. Annu. Rev. Plant Biol. *63*, 483–506.

Lee, K.M., and Tarn, W.Y. (2013). Coupling pre-mRNA processing to transcription on the RNA factory assembly line. RNA Biol. *10*, 380–390.

Li, X., and Manley, J.L. (2005). Inactivation of the SR protein splicing factor ASF/SF2 results in genomic instability. Cell *122*, 365–378.

Lin, S., Coutinho-Mansfield, G., Wang, D., Pandit, S., and Fu, X.D. (2008). The splicing factor SC35 has an active role in transcriptional elongation. Nat. Struct. Mol. Biol. *15*, 819–826.

Meinke, D., Muralla, R., Sweeney, C., and Dickerman, A. (2008). Identifying essential genes in *Arabidopsis thaliana*. Trends Plant Sci. *13*, 483–491.

Muller-McNicoll, M., Botti, V., de Jesus Domingues, A.M., Brandl, H., Schwich, O.D., Steiner, M.C., Curk, T., Poser, I., Zarnack, K., and

Neugebauer, K.M. (2016). SR proteins are NXF1 adaptors that link alternative RNA processing to mRNA export. Genes Dev. *30*, 553–566.

Onodera, Y., Haag, J.R., Ream, T., Costa Nunes, P., Pontes, O., and Pikaard, C.S. (2005). Plant nuclear RNA polymerase IV mediates siRNA and DNA methylation-dependent heterochromatin formation. Cell *120*, 613–622.

Onodera, Y., Nakagawa, K., Haag, J.R., Pikaard, D., Mikami, T., Ream, T., Ito, Y., and Pikaard, C.S. (2008). Sex-biased lethality or transmission of defective transcription machinery in *Arabidopsis*. Genetics *180*, 207–218.

Pauling, M.H., McPheeters, D.S., and Ares, M., Jr. (2000). Functional Cus1p is found with Hsh155p in a multiprotein splicing factor associated with U2 snRNA. Mol. Cell. Biol. *20*, 2176–2185.

Pontier, D., Yahubyan, G., Vega, D., Bulski, A., Saez-Vasquez, J., Hakimi, M.A., Lerbs-Mache, S., Colot, V., and Lagrange, T. (2005). Reinforcement of silencing at transposons and highly repeated sequences requires the concerted action of two distinct RNA polymerases IV in *Arabidopsis*. Genes Dev. *19*, 2030–2040.

Proudfoot, N.J., Furger, A., and Dye, M.J. (2002). Integrating mRNA processing with transcription. Cell *108*, 501–512.

Ream, T.S., Haag, J.R., Wierzbicki, A.T., Nicora, C.D., Norbeck, A.D., Zhu, J.K., Hagen, G., Guilfoyle, T.J., Pasa-Tolic, L., and Pikaard, C.S. (2009). Subunit compositions of the RNA-silencing enzymes Pol IV and Pol V reveal their origins as specialized forms of RNA polymerase II. Mol. Cell *33*, 192–203.

Ream, T.S., Haag, J.R., Pontvianne, F., Nicora, C.D., Norbeck, A.D., Pasa-Tolic, L., and Pikaard, C.S. (2015). Subunit compositions of *Arabidopsis* RNA polymerases I and III reveal Pol I- and Pol III-specific forms of the AC40 subunit and alternative forms of the C53 subunit. Nucleic Acids Res. *43*, 4163–4178.

Robert, H.S., Park, C., Gutierrez, C.L., Wojcikowska, B., Pencik, A., Novak, O., Chen, J., Grunewald, W., Dresselhaus, T., Friml, J., et al. (2018). Maternal auxin supply contributes to early embryo patterning in *Arabidopsis*. Nat. Plants *4*, 548–553.

Tan, E.H., Blevins, T., Ream, T.S., and Pikaard, C.S. (2012). Functional consequences of subunit diversity in RNA polymerases II and V. Cell Rep. *1*, 208–214.

ten Hove, C.A., Lu, K.J., and Weijers, D. (2015). Building a plant: cell fate specification in the early *Arabidopsis* embryo. Development *142*, 420–430.

Thomas, M.C., and Chiang, C.M. (2006). The general transcription machinery and general cofactors. Crit. Rev. Biochem. Mol. Biol. *41*, 105–178.

van Roon, A.M., Oubridge, C., Obayashi, E., Sposito, B., Newman, A.J., Seraphin, B., and Nagai, K. (2017). Crystal structure of U2 snRNP SF3b components: Hsh49p in complex with Cus1p-binding domain. RNA *23*, 968–981.

Wang, B.B., and Brendel, V. (2006). Molecular characterization and phylogeny of U2AF35 homologs in plants. Plant Physiol. *140*, 624–636.

Werner, F., and Grohmann, D. (2011). Evolution of multisubunit RNA polymerases in the three domains of life. Nat. Rev. Microbiol. *9*, 85–98.

Wu, H., Sun, S., Tu, K., Gao, Y., Xie, B., Krainer, A.R., and Zhu, J. (2010). A splicing-independent function of SF2/ASF in microRNA processing. Mol. Cell *38*, 67–77.

Wysocka-Diller, J.W., Helariutta, Y., Fukaki, H., Malamy, J.E., and Benfey, P.N. (2000). Molecular analysis of SCARECROW function reveals a radial patterning mechanism common to root and shoot. Development *127*, 595–603.

Xiao, R., Sun, Y., Ding, J.H., Lin, S., Rose, D.W., Rosenfeld, M.G., Fu, X.D., and Li, X. (2007). Splicing regulator SC35 is essential for genomic stability and cell proliferation during mammalian organogenesis. Mol. Cell. Biol. *27*, 5393–5402.

Yan, Q., Xia, X., Sun, Z., and Fang, Y. (2017). Depletion of *Arabidopsis* SC35 and SC35-like serine/arginine-rich proteins affects the transcription and splicing of a subset of genes. PLoS Genet. *13*, e1006663.

Yu, T.Y., Shi, D.Q., Jia, P.F., Tang, J., Li, H.J., Liu, J., and Yang, W.C. (2016). The *Arabidopsis* receptor kinase ZAR1 is required for zygote asymmetric division and its daughter cell fate. PLoS Genet. *12*, e1005933.

Zhang, Z., Tucker, E., Hermann, M., and Laux, T. (2017). A molecular framework for the embryonic initiation of shoot meristem stem cells. Dev. Cell *40*, 264–277.e4.

# Supplemental Information

# Arabidopsis JANUS Regulates Embryonic

# Pattern Formation through Pol II-Mediated

# Transcription of *WOX2* and *PIN7*

Feng Xiong, Hai-Hong Liu, Cun-Ying Duan, Bi-Ke Zhang, Guo Wei, Yan Zhang, and Sha Li
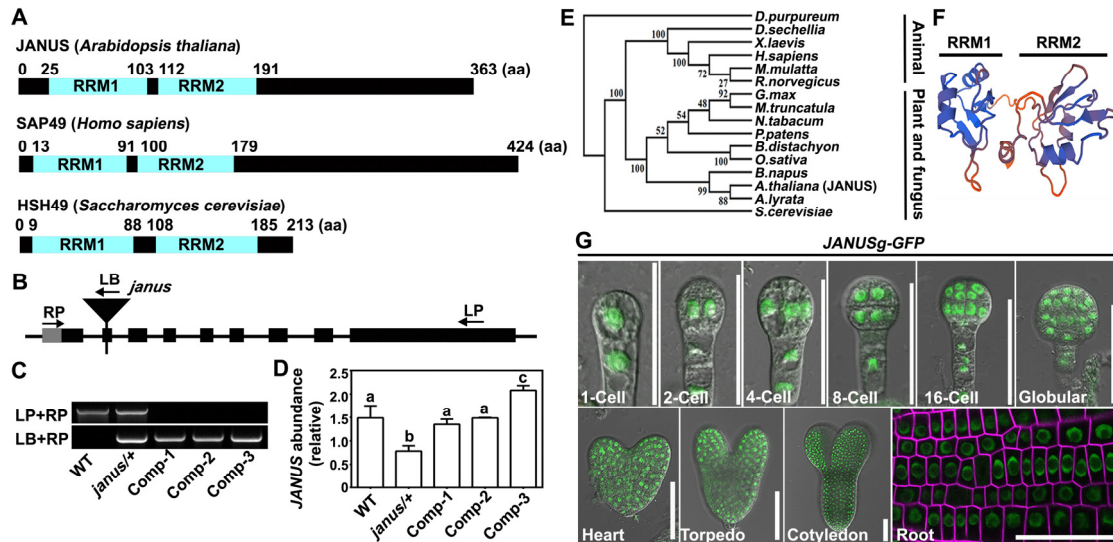
**Figure S1. JANUS is homologus to a component of the spliceosome and is present in the nucleus.**

(A) Domain organization of Arabidopsis JANUS and its yeast and human homologs. RRM, RNA recognition motif. Number of amino acid is on top.

(B) Schematic illustration of the *JANUS* genomic locus. LB, left border primer for T-DNA; LP, left primer; RP, right primer.

(C) Genotyping PCRs verify the genetic background of wild type (WT), *janus*/+, and three JANUSg-GFP;*janus* lines (Comp).

(D) Transcript analysis showing *JANUS* abundance. Results are means ± standard deviation (sd, n=3). Results are representative of three biological replicates. Different letters indicate significant difference (Tukey's multiple comparison test, $P<0.05$).

(E) Phylogenetic tree of JANUS and its homologs from *Arabidopsis lyrata* (XP_002886178.1), *Brachypodium distachyon* (XP_003574000.1), *Brassica napus* (CDY59539.1), *Dictyostelium purpureum* (XP_003287607.1), *Drosophila sechellia* (XP_002036808.1), *Glycin max* (XP_003540544.1), *Homo sapiens* (NP_005841.1), *Macaca mulatta* (NP_001248161.1), *Medicago truncatula* (XP_003600696.1), *Nicotiana tabacum* (XP_016437621.1), *Oryza sativa* (XP_015614791.1), *Physcomitrella patens* (XP_001764808.1), *Rattus norvegicus* (NP_001011951.1), *Saccharomyces cerevisiae* (AJT72224.1), and *Xenopus laevis* (NP_001080100.1).

(F) Structure model of JANUS N-terminus including both RRM motifs.

(G) Confocal laser scanning microscopy (CLSM) of JANUSg-GFP embryos at various developmental stages and root epidermal cells. Images shown are merges of the GFP channel and the transmission channel for embryos, and of the GFP channel and the RFP channel (FM4-64) for root cells. Scale bars, 20 µM.
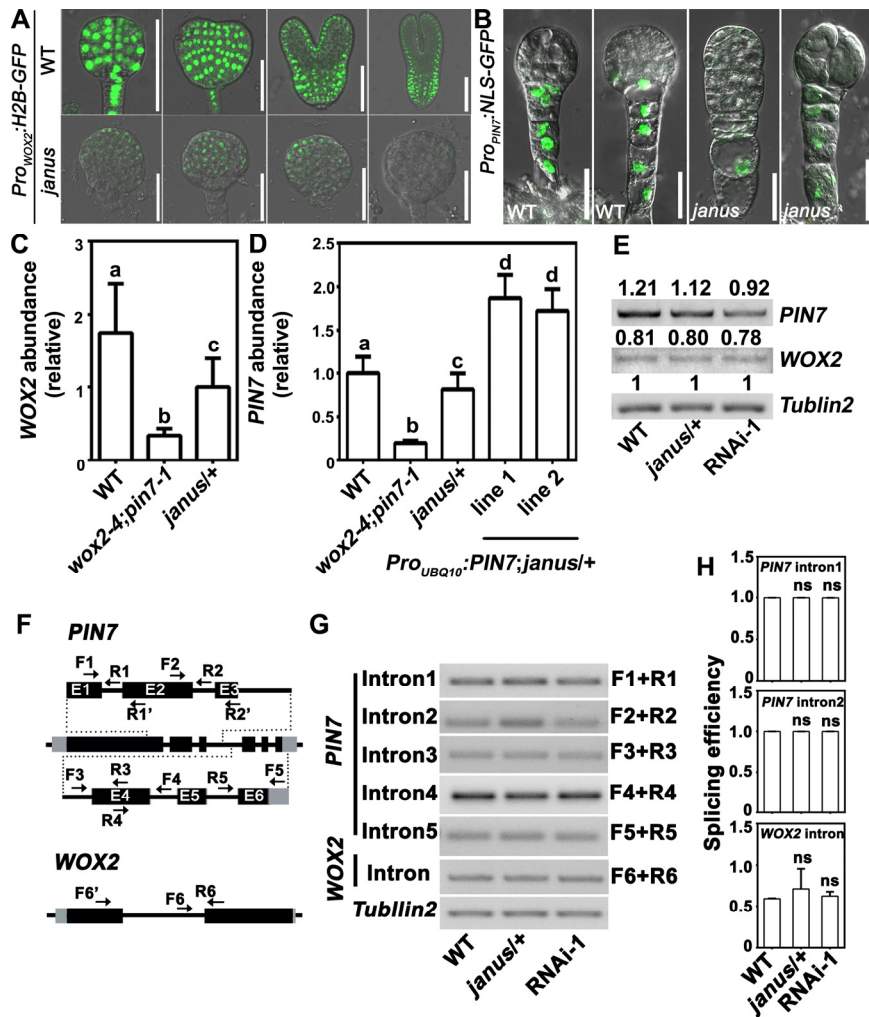
Related to Figure 1.

**Figure S2. JANUS mediates the expression but not RNA processing of *WOX2* and *PIN7*.**
(A) CLSM of a *Pro_WOX2*:H2B-GFP embryo at early developmental stages in wild type or in *janus*. Scale bars, 50 μm.
(B) CLSM of embryos from a different *Pro_PIN7*:NLS-YFP *or Pro_PIN7*:NLS-YFP;*janus*/+ plant. Scale bars, 50 μm.
(C) Transcript abundance of *WOX2* in WT, *wox2-4;pin7-1*, and *janus*/+ by qPCR.
(D) Transcript abundance of *PIN7* in WT, *wox2-4;pin7-1*, *janus*/+, and two lines of *Pro_UBQ10*:PIN7;*janus*/+ by qPCR. Results shown in (C) and (D) are means ± standard error (SEM) from three technical repeats. qPCRs were repeated three times with similar results. Different letters indicate significantly different groups (Tukey's multiple comparison test, P<0.05).
(E) RT-PCRs showing that both *PIN7* and *WOX2* have no alternative spliced forms in *janus*/+ or in *Pro_35S*:JANUS-RNAi. The above numbers indicate relative abundance. Experiments were repeated in three biological replicates with similar results.
(F) Schematic diagram of the genomic regions of *PIN7* and *WOX2.* Primers used for detecting intron retention and splicing efficiency are shown in the regions of interest. F, forward primer; R, reverse primer; Black box, exon; Gray box, UTR; Black line, intron.
(G) Intron retention that was detected via RT-PCRs shows no significant difference between WT, *janus*/+ and RNAi-1 siliques.
(H) Splicing efficiency of *PIN7* and *WOX2* was unaffected in *janus*/+ and RNAi-1 siliques. Splicing efficiency was calculated as the ratio of spliced to total (spliced + unspliced) transcripts for two representative *PIN7* introns and *WOX2* intron. Results are means ± SE from three experiments. ns indicates no significant difference (*t*-test, P>0.05).
Related to Figure 2.
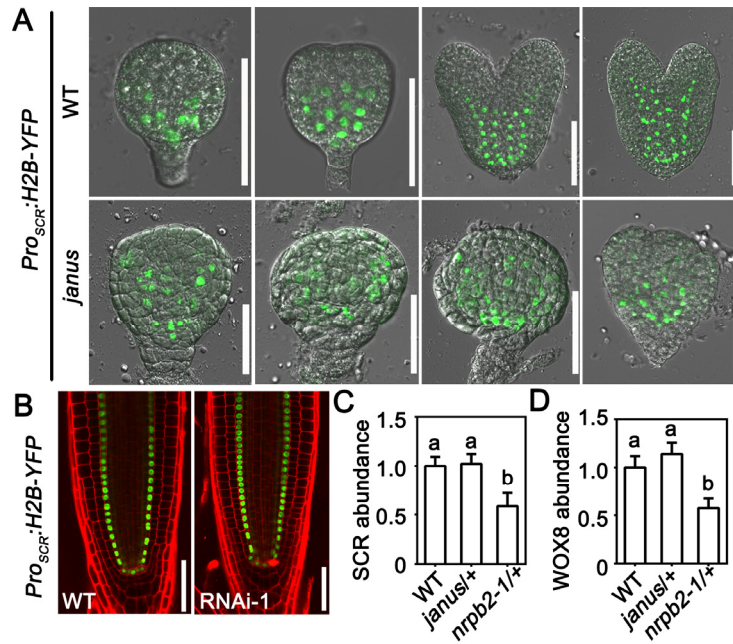
**Figure S3. The expression of *SCR* is reduced by functional loss of Pol II but not that of *JANUS*.**

(A) CLSM of *Pro_SCR*:H2B-YFP or *Pro_SCR*:H2B-YFP;*janus* embryos at various developmental stages. Images shown are merges of the GFP channel and the transmission channel. Scale bars, 50 μM.

(B) CLSM of a root from 4 DAG seedlings of *Pro_SCR*:H2B-YFP or *Pro_SCR*:H2B-YFP;*Pro_35S*:JANUS-RNAi. Images shown are merges of the GFP channel and the RFP channel (FM4-64). Scale bars, 50 μM.

(C-D) Relative transcript abundance of *SCR* (C) *and WOX8* (D) in the siliques of wild type, *janus/+*, or *nrpb2-1/+* by qPCRs. Results are means ± SEM from three technical repeats. Different letters indicate significantly different groups (Tukey's multiple comparison test, P<0.05).

Related to Figure 2 and Figure 4.
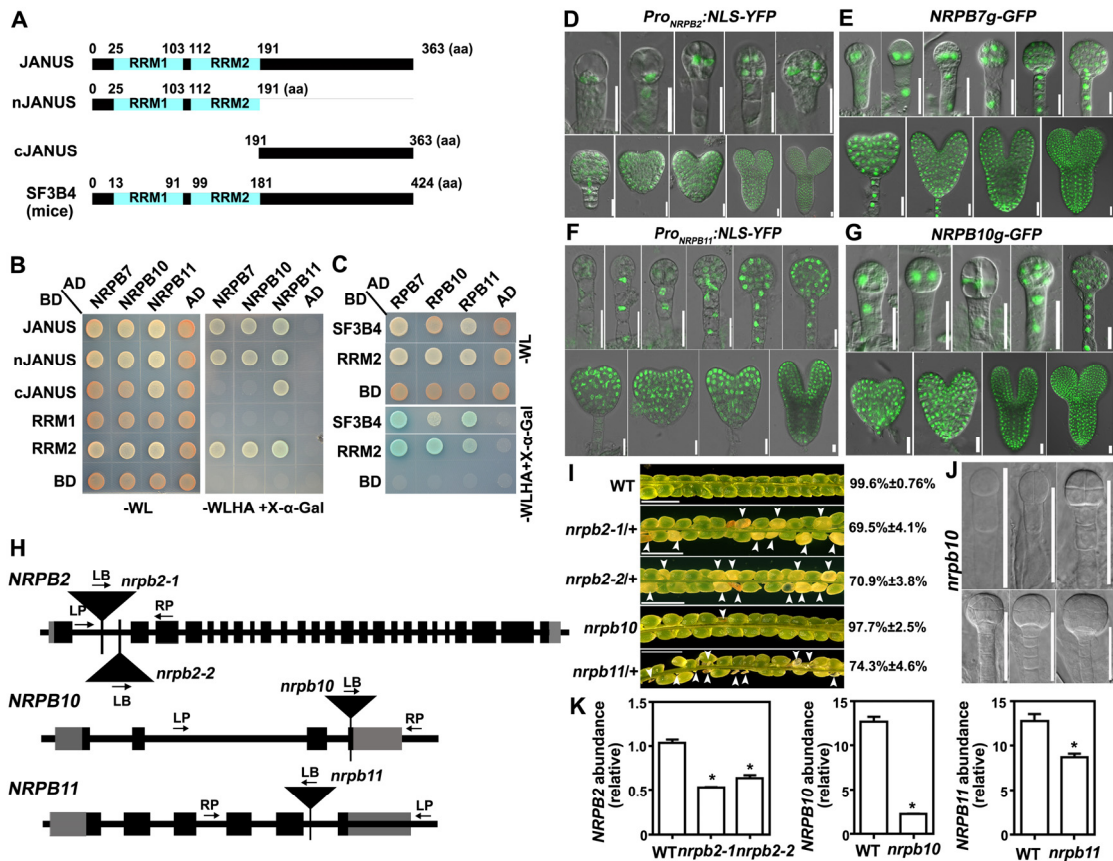
**Figure S4. Functional loss of Pol II components resulted in embryo lethality.**

(A) Domain organization of JANUS, its variants, and its mice homolog SF3B4. Number of amino acid is on top.

(B-C) Y2H assays demonstrating RRM1-dependent interaction between JANUS and Pol II components. Results shown are representative of three biological replicates.

(D-G) CLSM of $Pro_{NRPB2}$:NLS-YFP (D), *NRPB7g-GFP* (E), $Pro_{NRPB11}$:NLS-YFP (F), or *NRPB10g-GFP* (G) embryos during development. Images shown are merges of the GFP and transmission channels. Scale bars, 20 μM.

(H) Schematic illustration of the *NRPB2*, *NRPB10*, and *NRPB11* genomic loci. LB, left border primer for T-DNA; LP, left primer; RP, right primer.

(I) Seed set of different genotypes. Results are means ± sd (n=8). Scale bars, 1 mm.

(J) Embryogenesis of *nprb10* by ovule clearing. Scale bars, 50 μM.

(K) Relative transcript abundance of *NRPB2*, *NRPB10*, or *NRPB11* in corresponding mutants versus in wild type by qPCRs. Results are means ±SEM from three technical repeats. Experiments were repeated three times with similar results. Asterisks indicate significant difference (*t*-test, P<0.05).

Related to Figure 3.
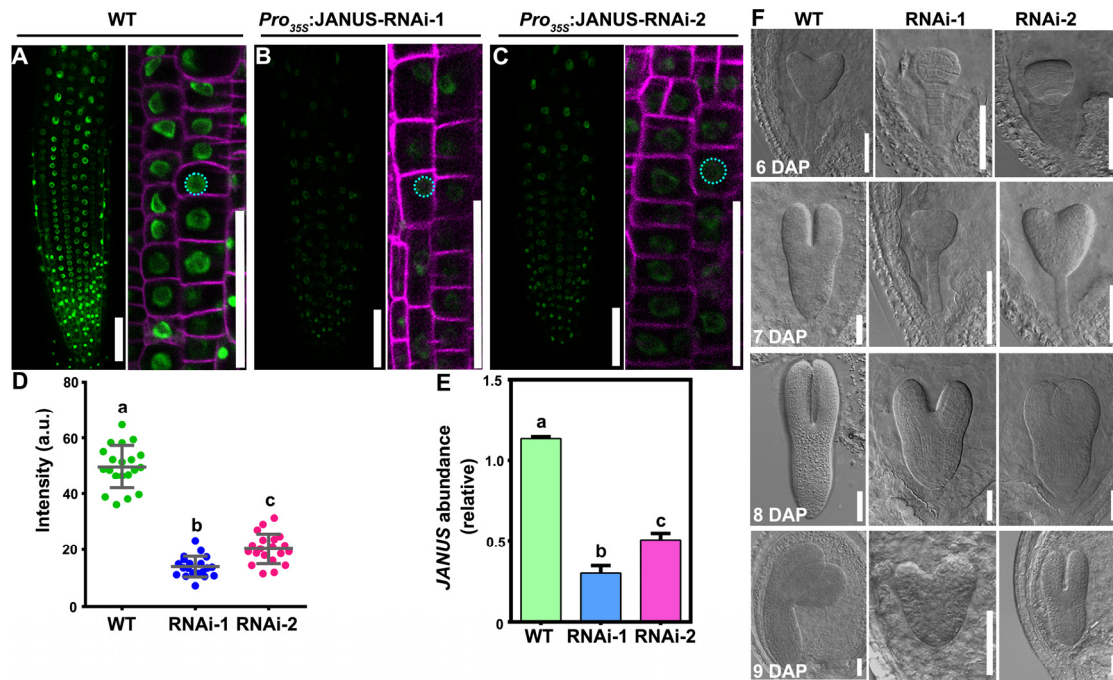
**Figure S5. JANUS-RNAi caused delayed embryogenesis.**

(A-C) CLSM of JANUSg-GFP (A), and two lines of *Pro35S*:JANUS-RNAi;JANUSg-GFP (B-C). Left images are whole root tips; right images are merges of the GFP channel (green, JANUS-GFP) and the RFP channel (magenta, FM4-64). Dotted circles indicate ROI.

(D) Quantification of fluorescence intensity. Results shown are average fluorescence intensities within a ROI, showing in (A-C). Scale bars, 20 μM.

(E) Relative transcript abundance of *JANUS* in WT or in *Pro35S*:JANUS-RNAi lines by qPCRs. Results are means ± SEM from three technical repeats. Experiments were repeated three times with similar results. Different letters indicate significantly different groups (Tukey's multiple comparison test, P<0.05).

(F) Representative stages of embryogenesis in wild type versus in two *Pro35S*:JANUS-RNAi lines. Scale bars, 50 μM.

Related to Figure 4.

**Table S1. *JANUS* loss-of-function does not compromise gametophytic transmission.**

| Parents | F1 progenies | | |
|---|---|---|---|
| Female X Male | Genotype | Expected ratio | Observed ratio |
| *janus*/+ X WT | WT : *janus*/+ | 1 : 1 | 66 : 67[a] |
| WT X *janus*/+ | WT : *janus*/+ | 1 : 1 | 83 : 79[a] |
| *janus*/+ X *janus*/+ | WT : *janus*/+: *janus* | 1 : 2 : 1 | 53 : 113[b] |

[a] Not significantly different from the segregation ratio 1:1 ($\chi^2$, P>0.05).
[b] Significantly different from the segregation ratio 1:2:1 ($\chi^2$, P>0.05).
Related to Figure 1.

**Table S2. Segregation of self-fertilized heterozygous Pol II mutants.**

| Parents | F1 progenies | | |
|---|---|---|---|
| Female X Male | Genotype | Expected ratio | Observed ratio |
| *nrpb2-1/+* X *nrpb2-1/+* | WT : *nrpb2-1/+*: *nrpb2-1* | 1 : 2 : 1 | 44 : 78 : 0[a] |
| *nrpb2-2/+* X *nrpb2-2/+* | WT : *nrpb2-2/+*: *nrpb2-2* | 1 : 2 : 1 | 36 : 65 : 0[a] |
| *nrpb10/+* X *nrpb10/+* | WT : *nrpb10/+*: *nrpb10* | 1 : 2 : 1 | 28 : 61 : 33[b] |
| *nrpb11/+* X *nrpb11/+* | WT : *nrpb11/+*: *nrpb11* | 1 : 2 : 1 | 15 : 33 : 0[a] |

[a] Significantly different from the segregation ratio 1:2:1 ($\chi^2$, P>0.05).
[b] Not significantly different from the segregation ratio 1:2:1 ($\chi^2$, P<0.05).
Related to Figure 3.

**Table S3. Oligos used in this study.**

| Application | | No. | 5'-3' sequences |
|---|---|---|---|
| Genotyping PCR | SALK LB | ZY1 | ATTTTGCCGATTTCGGAAC |
| | SAIL LB | ZY4 | GCTTCCTATTATATCTTCCCAAATTACCAATACA |
| | *janus/+* | ZY7860 | AGAAGCAATCACACCAAATGC |
| | | ZY7861 | TATAGGCCCATTAGAGACGGC |
| | | ZY7666 | GAATTGGTCCGAAACTGAGGCGAT |
| | *nrpb2-1/+* *nrpb2-2/+* | ZY7857 | TGGGAATTCGAAATTATGTGC |
| | | ZY7858 | CATTCTCCAAGCTCTGTCAGG |
| | *nrpb10* | ZY7892 | TGGAAGAGACTATGTCCTGCC |
| | | ZY7893 | TATGTTCCCTTAAGAACGGGG |
| | *nrpb11/+* | ZY7894 | GAGAGTATGGGCTGGTGATTG |
| | | ZY7895 | AGAGCCTGTTGCTTTGAATTG |
| | *wox2-4* | ZY8654 | CTTACTTCAATCGCCTCCTCC |
| | | ZY8655 | AGAATGTCTATGTCGGCCTCC |
| | *pin7-1* | ZY2931 | TGCCTAACGGACTACACAAGC |
| | | ZY2932 | ACCGCCATCGCAAAAGTC |
| Cloning | *JANUS* | ZY7639 | CACCATGACGACTCGAATCGCTCCTG |
| | | ZY7642 | TCAACCTTGGTGTGGTGGTGGT |
| | *nJANUS* | ZY7639 | CACCATGACGACTCGAATCGCTCCTG |
| | | ZY7640 | TCACTTGTATGCGTAAGAGACTGTGA |
| | *cJANUS* | ZY7641 | CACCATGAAAGACACCAAAGGAGAG |
| | | ZY7642 | TCAACCTTGGTGTGGTGGTGGT |
| | *JANUS-RRM1* | ZY8676 | CACCATGGCCACTGTTTACGTCGGTGGTC |
| | | ZY8677 | TTATTGAGATGCCTTGTTAACACG |
| | *JANUS-RRM2* | ZY8678 | CACCATGGCTAACCTTTTCATTGGAAACC |
| | | ZY8679 | TTACTTGTATGCGTAAGAGACTGTG |
| | *NRPB2* | ZY7373 | TAAGAAGGAGCCCTTCACCAAGCTTATGGAGTACAACGAATACGAACCTG |
| | | ZY7374 | GGTCGGCGCGCCCACCCTTCTCGAGTCACTGTCTGCCTTTAGCCGA |
| | *NRPB3* | ZY7499 | CACCATGGACGGTGCCACATACCAAAG |
| | | ZY7500 | TCATCCTCCACGCATATGGGCA |
| | *NRPB4* | ZY7479 | CACCATGTCCGGAGAAGAAGAAGAG |
| | | ZY7480 | CTACTCGAATCTCTTGACAAGTG |
| | *NRPB5* | ZY7481 | CACCATGTTGACGGAAGAGGAGCTC |
| | | ZY7482 | GGCTTATACAACATAACGATAGG |
| | *NRPB6a* | ZY7483 | CACCATGGCTGACGAAGATTACAAC |
| | | ZY7484 | TCAATCACCACCAACTTGACG |
| | *NRPB7* | ZY7485 | CACCGTCGAGATGTTTTTCCACATAG |
| | | ZY7486 | TTATGCCGCTGCAGGGTCGTTTATG |
| | *NRPB8a* | ZY7487 | CACCATGGCGAGCAATATCATCTTG |
| | | ZY7488 | TCACAGCTTCCTCATGAGTAG |
| | NRPB8b | ZY7489 | CACCATGGCGAGCAATATTATCATGTTCG |
| | | ZY7490 | TCAAAGCTTCCTCATGAGTAGAAAG |
| | *NRPB9a* | ZY7192 | CACCATGAGTACTATGAAATTTTGCCGCG |
| | | ZY7193 | TTATTCTCTCCAGCGATGACCACA |
| | *NRPB9b* | ZY7491 | CACCGATTCTGCGAAGATGAGTACTATG |
| | | ZY7492 | CTATTCTCTCCAACGGTGACTAC |
| | *NRPB10* | ZY7497 | CACCATGATCATCCCTGTTCGTTGC |
| | | ZY7498 | CTAACTGTTGTCTGATTTCTCCAG |
| | *NRPB11* | ZY7493 | CACCATGAATGCTCCCGAACGATATGAGC |
| | | ZY7494 | ACTCCAAGTTCCTTAAAACTGATTCG |
| | *NRPB12* | ZY7495 | CACCATGGATCCAGCGCCCGAACC |
| | | ZY7496 | TCAGCGAGCTTCGTATTGAAC |

| | | | |
|---|---|---|---|
| | *PIN7* CDS | ZY7986 | CACCATGATCACATGGCACGACCTCTAC |
| | | ZY7987 | TTATAGCCCGAGTAAAATGTAGT |
| | *JANUS* genomic | ZY6987 | ACCTTGGTGTGGTGGTGGTGGA |
| | | ZY6988 | CACCCGCTTGACAACTCTAGTCACGTTAG |
| | *JANUS* RNAi | ZY7194 | GGGGACAAGTTTGTACAAAAAAGCAGGCTATGACGACTCGAATCGCTCCTG |
| | | ZY7195 | GGGGACCACTTTGTACAAGAAAGCTGGGTATAGGAGTCATAGCTGATGAAACCA |
| | *Pro*PIN7 | ZY7984 | CACCGTGAGCGGTGTAGACACAAAC |
| | | ZY7985 | ATTGTTGTTCGCCGGAGTGGCA |
| | *Pro*NRPB2 | ZY7477 | CACCTACAGCCACACGGGTTCAGAGAAGT |
| | | ZY7478 | TCTCACTCTCTGAAGATTAGAGCACA |
| | *Pro*NRPB11 | ZY7575 | CACCCTATCACCGAGGAGGAGAATATG |
| | | ZY7576 | GGCTTAATCGGAGATTTCAAGCT |
| | *NRPB7g* | ZY7571 | CACCGTCTTGTCTAGCTACTTTTGCTCTCG |
| | | ZY8235 | TGCCGCTGCAGGGTCGTTTATG |
| | *NRPB10g* | ZY7573 | CACCTCTCGTAAGCGTAGAGATCTTCA |
| | | ZY8236 | ACTGTTGTCTGATTTCTCCAG |
| | *SF3B4* (Mice) | ZY9179 | CACCATGGCTGCCGGACCGATCTCCGAA |
| | | ZY9180 | TTACTGAGGAAGTGGGCCCCGAAGAG |
| | *SF3B4 RRM2* (Mice) | ZY9183 | CACCATGGCCAACATTTTCATTGGAAATCTGG |
| | | ZY9184 | TCACTTGAAGGCATAAGACACAGTGATA |
| | *RPB7* (Mice) | ZY9185 | CACCATGTTTTATCACATTTCCCTGGAGC |
| | | ZY9186 | TCAGCTCACGAGCCCCAAGTAGT |
| | *RPB10* (Mice) | ZY9187 | CACCATGATCATCCCGGTGCGCTGCTT |
| | | ZY9188 | TCACTTCTCTAGGGGTGCATAGTTC |
| | *RPB11* (Mice) | ZY9189 | CACCATGAACGCTCCTCCGGCCTTCGA |
| | | ZY9190 | CTACTCAATTCCTTCTTGCTTGTCC |
| RT-PCR | *PIN7* | ZY7986 | CACCATGATCACATGGCACGACCTCTAC |
| | | ZY7987 | TTATAGCCCGAGTAAAATGTAGT |
| | *WOX2* | ZY7880 | CACCATGGAAAACG AAGTAAACGC AG |
| | | ZY7881 | TTACAACCCATTACCATTACTATC |
| | *TUBLLIN2* | Tub2 U | GGTATCCAGGTCGGAAATGC |
| | | Tub2 D | TCCCGTAGTCAACAGAAAGT |
| qRT-PCR | ChIP *PIN7* Region a | ZY8596 | TGGACAGGGTGGCTTAAAAGTGAGA |
| | | ZY8597 | GTGCAATGCAAGATCATATTCGCCG |
| | ChIP *PIN7* Region b | ZY8598 | CTTCTCCTTCTCTCTCTCTCTC |
| | | ZY8599 | ATTGTTGTTCGCCGGAGTGGCAAA |
| | *WOX2* | ZY8592 | AGGAGCGCATGGCTTACTTCA |
| | | ZY8593 | TTCTCGTAGCCACCACTTGGA |
| | *WOX8* | ZY9725 | AACCTATCATCTTCCTTTTCCTCAG |
| | | ZY9727 | AGGTGGGTTAATAGTACCGGAATTG |
| | *SCR* | ZY9594 | GATGTCACTGGCTCTGATGCACACA |
| | | ZY9595 | TCGATAATAGCTGCTGTTCCACGAC |
| | *PIN7* | ZY8594 | GTGGGATGTGGCAATGCCTAA |
| | | ZY8595 | TCCAATAGCCATTGCTGCCAC |
| | *JANUS* | QRT U | TTGGCAGCCACAAATCCAACTGC |
| | | QRT D | GCTGTGTTGTTGTGGCTGAGATG |
| | *GAPDH* | ZY687 | TTGATCTTTTGTGTT ATTCCCTTCT |
| | | ZY688 | CATCATCCTCGGTGTATCCAA |
| | *ACT2* | ZY313 | CGTGACCTTACTGATTAC |
| | | ZY314 | TTCTCCTTGATGTCTCTT |
| Splicing of *PIN7* and *WOX2* | *PIN7* intron1 | F1 | CAAGTTGATAATGGAGCCAATGAA |
| | | R1 | CAGTTTGAGATTTGTGTCCATATG |
| | | R1' | GTTAGGCACTTCCTTTACCCTCT |

| | | | |
|---|---|---|---|
| | *PIN7* intron2 | F2 | CTGATATTGATAATGGTGTGGAG |
| | | R2 | TCATCACTCTAATCAAATCTCACAA |
| | | R2' | CCAAACTGAACATTGCCATACCAAG |
| | *PIN7* intron3 | F3 | CATGTATTGCATCATTCAGCACTTG |
| | | R3 | CTGGTCCAGTAAAGAATCTCACC |
| | *PIN7* intron4 | F4 | CCAAATCTTGTGGTAACGTTGTAG |
| | | R4 | CTGGTCCAGTAAAGAATCTCACC |
| | *PIN7* intron5 | F5 | GTTGATTCTTATGTGTATTATTGCAG |
| | | R5 | GCGTTCCACTAATCTTGGAATTATC |
| | *WOX2* intron | F6 | CCAGTTTTGGCCATTTATCGCTGAG |
| | | R6 | GTAAATAGTACGGACTGACACAACCCA |
| | | F6' | TGGTTCCAGAACCATAAGGCTAGG |

Related to Figure 1-5.

**Transparent Methods**
**Plant materials and growth conditions**
Arabidopsis thaliana ecotype Columbia-0 (Col-0) was used as wild type for all experiments in this study. T-DNA insertion mutants of *JANUS* (SALK_008993 as *janus*), *NRPB2* (CS16201 as *nrpb2-1*, CS16202 as *nrpb2-2*), *NRPB10* (SALK_114301C as *nrpb10-1*), and *NRPB11* (SALK_100563 as *nrpb11-1)*, *WOX2* (SALK_114607 *as wox2-4*), *PIN7* (SALK_044687 *as pin7-1*) were verified by PCRs. Plant marker lines carring *DR5rev:GFP* (Ulmasov et al., 1997), *PIN7:GFP* (Blilou et al., 2005), *Pro_{WOX5}:GFP* (Blilou et al., 2005), *Pro_{WOX2}:DsRed2/Pro_{WOX8gΔ}:NLS-vYFP3* (Yu et al., 2016), *Pro_{SCR}:H2B-YFP* (Heidstra et al., 2004)*, Pro_{WOX2}:H2B-GFP* (Gooh et al., 2015) were described. The marker lines were crossed with *janus/+*, *Pro_{35S}:JANUS-RNAi*, or *nrpb2-1/+* and verified by PCRs and by fluorescence imaging. Seedlings and plants were grown in a growth chamber at 20 ± 2 ℃ under long-day condition (16 h light/8 h dark).

**DNA manipulation**
All constructs were generated using the Gateway technology (Invitrogen) except where noted. Entry clones were generated in the pENTR/D/TOPO vector (Invitrogen). The coding sequences were cloned with the following primers: ZY7639/ZY7642 for *JANUS*, ZY7639/ZY7640 for N-terminal of *JANUS* (1-191aa), ZY7641/ZY7642 for C terminal of *JANUS* (192-363aa), ZY8676/ZY8677 for *JANUS-RRM1* (25-103aa), ZY8678/ZY8679 for *JANUS-RRM2* (112-191aa), ZY7373/ZY7374 for *NRPB2*, ZY7499/ZY7500 for *NRPB3*, ZY7479/ZY7480 for *NRPB4*, ZY7481/ZY7482 for *NRPB5*, ZY7483/ZY7484 for *NRPB6a*, ZY7485/ZY7486 for *NRPB7*, ZY7487/ZY7488 for *NRPB8a*, ZY7489/ZY7490 for *NRPB8b*, ZY7192/ZY7193 for *NRPB9a*, ZY7491/ZY7492 for *NRPB9b*, ZY7497/ZY7498 for *NRPB10*, ZY7493/ZY7494 for *NRPB11*, ZY7495/ZY7496 for *NRPB12*, ZY7880/ZY7881 for *WOX2* and ZY7986/ZY7987 for *PIN7*. Destination vectors used for expressing GFP-translational fusions *in planta* are *Pro_{UBQ10}*:GFP-GW and *Pro_{UBQ10}*:GW (Zhang et al., 2018), for Y2H are pDEST-GBKT7 and pDEST-GADT7 (Invitrogen), for BiFC are pSITE::cEYFP-C1 and pSITE-nEYFP-C1 (Martin et al., 2009).

A 3875 bp sequence containing the 1489 bp upstream of the *JANUS* translation start codon and the genomic fragment of *JANUS* without the stop codon was amplified with the primer pair ZY6987/ZY6988. The entry vector containing JANUSg was used in an LR reaction with the destination vector GW:GFP (Zhou et al., 2013) to generate JANUSg-GFP.

To generate *Pro_{35S}*:JANUS-RNAi, a 500 bp fragment from the N-terminus of *JANUS* was amplified with the primer pair ZY7194/ZY7195. The fragment was cloned into *Pro_{35S}*:GW-RNAi vector (Wang et al., 2017) via a BP reaction (invitrogen) to generate *Pro_{35S}*:JANUS-RNAi.

For the promoters of *PIN7*, *NRPB2*, and *NPRB11*, a 2175 bp, a 1904 bp, or a 1973 bp sequence upstream of the translational start codon of the respective gene was amplified with primer pairs, ZY7984/ZY7985 for *PIN7*, ZY7477/ZY7478 for *NRPB2* and ZY7575/ZY7576 for *NRPB11*. The entry vectors were used in LR reactions with the destination vector GW::NLS-YFP (Wang et al., 2017) to generate *Pro_{NRPB2}:NLS-YFP* or *Pro_{NRPB11}:NLS-YFP*. For the expression analysis of NRPB7 and NRPB10, a 2924 bp or a 3277 bp genomic sequence of the respective gene was amplified with primer pairs, ZY7571/ZY8235 for *NRPB7* and ZY7573/ZY8236 for *NRPB10*. The entry vectors were used in LR reactions with the destination vector GW::GFP (Zhou et al., 2013) to generate *NRPB7g-GFP* or *NRPB10g-GFP*, respectively.

PCR amplifications were performed with Phusion hot-start high-fidelity DNA polymerase with the annealing temperature and extension times recommended by the manufacturer. All entry vectors were sequenced. All primers are listed in Supplemental Table 3.

**PCRs, RNA extraction, RT-PCRs, and qPCRs**
Genotyping PCRs of *janus*, *nrpb2-1*, *nrpb2-2*, *nrpb10*, *nrpb11*, *wox2-4*, and *pin7-1* were performed using the following primers: ZP7860/ZP7861 for the wild-type copy of *JANUS*, ZP1/ZP7861 for *janus*; ZP7857/ZP7858 for the wild-type copy of *NRPB2*, ZP4/ZP7858 for *nrpb2-1* and *nrpb2-2*; ZP7892/ZP7893 for the wild-type copy of *NRPB10*, ZP1/ZP7893 for *nrpb10*; ZP7894/ZP7895 for the wild-type copy of *NRPB11*, ZP1/ZP7895 for *nrpb11-1*;

ZP8654/ZP8655 for the wild-type copy of *WOX2*, ZP1/ZP8655 for *wox2-4*; ZP2931/ZP2932 for the wild-type copy of *PIN7*, ZP1/ZP2932 for *pin7-1*. Genotyping PCRs of the JANUSg-GFP;*janus* were performed using the following primers: ZP7860/ZP7666 for the endogenous *JANUS* and ZP7190/ZP7191 for the transgene. *ACT2* was amplified with the primer pair ZP16/ZP17.

For qRT-PCRs analyzing the expression of *JANUS*, *SCR*, and *WOX8*, total RNAs were isolated from siliques (2-3 days after anthesis). For qRT-PCRs analyzing the expression of *WOX2* and *PIN7*, total RNAs were isolated from seedlings at 12 days after germination (DAG) of wild type and *Pro35S*:JANUS-RNAi plants. For RT-PCRs analyzing the splicing pattern of *WOX2* and *PIN7*, total RNAs were isolated from siliques (2-3 days after anthesis) of wild type, *janus*/+, and *Pro35S*:JANUS-RNAi plants. Total RNAs were isolated using a Qiagen RNeasy plant mini kit according to manufacture's instructions. Oligo(dT)-primed cDNAs were synthesized using Superscript III reverse transcriptase with on-column DNase II digestion (Invitrogen). The qRT-PCRs were performed with the Bio-Rad CFX96 real-time system using SYBR Green real-time PCR master mix (Toyobo) as described (Zhou et al., 2013). *GAPDH* and *ACT2* were used as a quantitative control for qRT-PCR. All experiments were repeated in three biological replicates with similar results. All primers are listed in Supplemental Table 3.

### Ovule clearing
Ovules were dissected from siliques and cleared with Hoyer's solution following the protocol described previously (Yadegari et al., 1994). A Zeiss LSM880 laser scanning microscope with differential interference contrast (DIC) optics was used to capture the images of cleared embryos.

### Protein interaction assays
Y2H assays were performed as described (Park et al., 2014) with slight modifications. Briefly, different combinations of bait and prey vectors were co-transformed into the Y2HGold yeast strain (Clontech). Positive interactions were determined by the appearance of blue colonies after 3 days on YSD-WHLA supplemented with 80 mg/l X-α-Gal. BiFC by Agrobacterium infiltration was performed as described, in which a P19 protein was used to suppress gene silencing (Park et al., 2014). U1-70K-mCherry was used as the nuclear marker (Wang et al., 2012). Confocal imaging was performed 48 hours after infiltration.

### Fluorescence imaging and quantification
Fluorescence images were captured using a Zeiss LSM880 laser scanning microscope with a 20 or 40/1.3 oil objective. Fluorescence of GFP, YFP, mCherry and PI staining was captured using the following exitation/emission settings: 488 nm/505-550 nm for GFP, 514 nm/530–590 nm for YFP, 561 nm/600–650 nm for mCherry and PI staining. Image processing was performed with the Zeiss LSM image processing software (Zeiss). Embryos of the *ProWOX2*:DsRed2;*ProWOX8gΔ*:NLS-vYFP3 or the *ProWOX2*:DsRed2;*ProWOX8gΔ*:NLS-vYFP3;*janus*/+ plants at the two-cell stage and at the globular stage were imaged with CLSM. Regions of interest (ROI) was defined as the nuclear region. Quantification of fluorescence intensity was performed using 10 two-cell stage embryos or globular stage embryos. Roots of 10 days after germination (DAG) seedlings of JANUSg-GFP, *ProWOX2*:H2B-GFP, or *PIN7:GFP* in wild type versus in the *Pro35S:JANUS-RNAi* background were images with CLSM. ROI was defined as the nuclear region for JANUSg-GFP and *ProWOX2*:H2B-GFP, or as a PM domain for *PIN7:GFP*. Quantification of fluorescence intensity was performed using 20 roots involving 40 to 60 cells. Quantification of fluorescence intensity was performed with ImageJ. Statistical analyses were done by Student's *t*-test.

### Chromatin immunoprecipitation (ChIP)
ChIP assays were performed as described (Saleh et al., 2008). Wild-type and *Pro35S:JANUS-RNAi* seedlings at 12 DAG of 2 g were harvested in a cross-linking buffer (0.4 M sucrose, 10 mM Tris-HCl (pH8.0), 1 mM PMSF, 1 mM EDTA, 1% formaldehyde) for 10 min using vacuum infiltration and then halted in 2 M glycine. After the addition of 5 μg Pol II antibodies (Abcam) to the chromatin and incubation at 4℃ overnight, the agarose beads of protein A and protein G were added and incubated at 4℃ for 2.5 h. After reverse cross-linking, DNA was purified and dissolved in 20 μl water. The immuno-precipitated DNA was diluted and then quantified by real-time PCR. Real-time PCR data of Pol II were normalized to Actin. The

enrichment of Pol II at the genomic locus of *PIN7* was given as the ratio of (Pol II *PIN7*/input *PIN7*) to (Pol II *Actin*/input *Actin*). ZY8596/ZY8597 for *PIN7* fragment A; ZY8598/ZY8599 for *PIN7* fragment B. Primers are listed in Supplemental Table 3.

## Detection of alternative splicing
Primers designed within the introns were used in RT-PCR. Splicing efficiency was measured as described (Mahrez et al., 2016) where a primer in an exon was combined with a primer in a neighboring intron (for the unspliced transcript) or covering the splicing junction (for the spliced transcript).

## Phylogenetic analysis and homology modeling
Protein homologs of *JANUS* were identified by performing BLASTP searches against the NCBI protein database (http://www.ncbi.nlm.nih.gov/) using default parameters. Multiple sequence alignment of JANUS homologs in various species was generated with ClustalX1.83. Then the alignment result was used to build the phylogenetic tree using MEGA5.1. The neighbor-joining method was used with a bootstrap (1000 replicates) test of phylogeny. The predicted structural models of JANUS were obtained by SWISS-MODEL (http://www.swissmodel.expasy.org/), while the crystal structure of human SAP49 was used as the template. The finished models were visualized using Swiss-Pdb Viewer 4.1.0.

## Accession numbers
Sequence data in this article can be found in TAIR (The Arabidopsis Information Resource) under these accession numbers: *JANUS* (At2g18510), *NRPB1* (At4g35800), *NRPB2* (At4g21710), *NRPB3* (At2g15430), *NRPB4* (At5g09920), *NRPB5* (At3g22320), *NRPB6a* (At5g51940), *NRPB7* (At5g59180), *NRPB8a* (At1g54250), *NRPB8b* (At3g59600), *NRPB9a* (At3g16980), *NRPB9b* (At4g16265), *NRPB10* (At1g11475), *NRPB11* (At3g52090), *NRPB12* (At5g41010), *PIN7* (At1g23080), *SCR* (At3g54220), *WOX2* (At5g59340), *WOX5* (At3g11260), *WOX8* (At5g45980).

## Supplemental References
Gooh, K., Ueda, M., Aruga, K., Park, J., Arata, H., Higashiyama, T., and Kurihara, D. (2015). Live-cell imaging and optical manipulation of *Arabidopsis* early embryogenesis. Dev. Cell 34, 242-251.

Heidstra, R., Welch, D., and Scheres, B. (2004). Mosaic analyses using marked activation and deletion clones dissect *Arabidopsis* SCARECROW action in asymmetric cell division. Genes Dev. 18, 1964-1969.

Mahrez, W., Shin, J., Munoz-Viana, R., Figueiredo, D.D., Trejo-Arellano, M.S., Exner, V., Siretskiy, A., Gruissem, W., Kohler, C., and Hennig, L. (2016). BRR2a affects flowering time via FLC splicing. PLoS Genet. 12, e1005924.

Martin, K., Kopperud, K., Chakrabarty, R., Banerjee, R., Brooks, R., and Goodin, M.M. (2009). Transient expression in *Nicotiana benthamiana* fluorescent marker lines provides enhanced definition of protein localization, movement and interactions in planta. Plant J. *59*, 150-162.

Park, S.J., Jiang, K., Tal, L., Yichie, Y., Gar, O., Zamir, D., Eshed, Y., and Lippman, Z.B. (2014). Optimization of crop productivity in tomato using induced mutations in the florigen pathway. Nat. Genet. *46*, 1337-1342.

Saleh, A., Alvarez-Venegas, R., and Avramova, Z. (2008). An efficient chromatin immunoprecipitation (ChIP) protocol for studying histone modifications in *Arabidopsis* plants. Nat. Protoc. *3*, 1018-1025.

Ulmasov, T., Murfett, J., Hagen, G., and Guilfoyle, T.J. (1997). Aux/IAA proteins repress expression of reporter genes containing natural and highly active synthetic auxin response elements. Plant Cell *9*, 1963-1971.

Wang, J.G., Feng, C., Liu, H.H., Feng, Q.N., Li, S., and Zhang, Y. (2017). AP1G mediates vacuolar acidification during synergid-controlled pollen tube reception. Proc. Natl. Acad. Sci. U S A *114*, E4877-e4883.

Wang, X., Wu, F., Xie, Q., Wang, H., Wang, Y., Yue, Y., Gahura, O., Ma, S., Liu, L., Cao, Y.*, et al.* (2012). SKIP is a component of the spliceosome linking alternative splicing and the circadian clock in *Arabidopsis*. Plant Cell *24*, 3278-3295.

Yadegari, R., Paiva, G., Laux, T., Koltunow, A.M., Apuya, N., Zimmerman, J.L., Fischer, R.L., Harada, J.J., and Goldberg, R.B. (1994). Cell differentiation and morphogenesis are uncoupled in *Arabidopsis raspberry* embryos. Plant Cell *6*, 1713-1729.

Zhang, W.T., Li, E., Guo, Y.K., Yu, S.X., Wan, Z.Y., Ma, T., Li, S., Hirano, T., Sato, M.H., and Zhang, Y. (2018). *Arabidopsis* VAC14 is critical for pollen development through mediating vacuolar organization. Plant Physiol. *177*, 1529-1538.

Zhou, L.Z., Li, S., Feng, Q.N., Zhang, Y.L., Zhao, X., Zeng, Y.L., Wang, H., Jiang, L., and Zhang, Y. (2013). Protein S-ACYL Transferase10 is critical for development and salt tolerance in *Arabidopsis*. Plant Cell *25*, 1093-1107.